

(200)
R290
no. 84-515



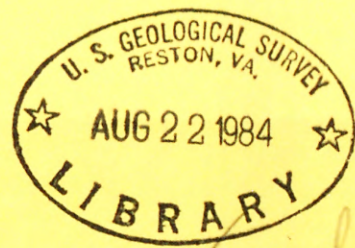
UNITED STATES DEPARTMENT OF THE INTERIOR

GEOLOGICAL SURVEY

Liquefaction Potential in the Central Mississippi Valley

by

Stephen F. Obermeier
U.S. Geological Survey
926 National Center
Reston, Virginia
22092



For avail

Open-File Report 84-515

This report (map) is preliminary and has not been reviewed for conformity with U.S. Geological Survey editorial standards and stratigraphic nomenclature.

Liquefaction Potential in the Central Mississippi Valley

by

Stephen F. Obermeier

U.S. Geological Survey

926 National Center

Reston, Virginia

22092

Open-file report
(Geological Survey
(U.S.))

Abstract

Liquefaction-induced ground failure caused by the 1811-12 New Madrid earthquakes was commonplace over large areas, even far from the epicenters. Recurrence of such strong earthquakes would undoubtedly cause severe liquefaction again, and lead to the destruction of many bridges and buildings in the central Mississippi Valley.

Methods for determining regional liquefaction potential are generally based on evaluating the severity of ground shaking by some combination of earthquake accelerations, magnitudes, or intensities, together with an assessment of the properties of the sediments. The severity of ground shaking is based either directly or indirectly on stress (i.e., acceleration) level and the number of applications of high stress. Some estimated accelerations are presented for the 1811-12 earthquakes, based on the pattern of sand boils from those earthquakes and mechanical properties of sands in the region of liquefaction. From those 1811-12 acceleration data and modern seismic data, accelerations

355279

can be estimated for any magnitude earthquake. Because there are so few data on strong earthquakes in this particular area, though, it is recommended that other methods also be used, preferably based on data from the 1811-12 earthquakes and other historical data in the central Mississippi Valley. The final judgment of liquefaction potential should be based on more than one method.

Sediments in the central Mississippi Valley susceptible to liquefaction are generally restricted to sands and silts. There are many large terraces and flood plains in the central Mississippi Valley region which contain moderately dense to loose clean sands and silty sands. Evaluation of their properties and relating these properties to liquefaction susceptibility is reasonably easy and straightforward. However, there are also many thick glacial lake deposits, eolian deposits, and reworked eolian deposits made up of silt-rich materials of highly varying liquefaction potential. Field methods for assessing their properties are very crude, and there appear to be so few laboratory data that there are no guidelines based on simple criteria such as void ratio, cohesion, and plasticity characteristics.

Liquefaction Potential in the Central Mississippi Valley

- I Introduction
- II Overview of Liquefaction
 - A. Conditions for liquefaction
 - B. Materials prone to liquefaction
 - C. Consequences of liquefaction
 - D. Engineering evaluation of liquefaction potential
- III Liquefaction and Historical Earthquakes
 - A. 1811-12 earthquakes
 - 1. Alluvium in St. Francis and Western Lowlands Basins
 - 2. Sand boil deposits in St. Francis Basin
 - 3. Energy release center
 - 4. Accelerations in alluvium
 - 5. Accelerations in bedrock
 - 6. Farthest liquefaction
 - B. Other historical earthquakes
 - C. Earthquake intensity and liquefaction
- IV Critique of Historical and Other Data
 - A. Accelerations
 - B. Magnitudes
 - C. Intensities
- V Liquefaction Susceptibility and Geologic Origin
 - A. Braided stream and meander belt deposits
 - B. Glacial lake deposits

C. Flood plains, exclusive of very young sediments

D. Very young sediments

E. Eolian deposits

F. Reworked eolian deposits

VI Summation

VII References Cited

List of Figures

1. Map of the northern Mississippi Embayment of the Gulf Coastal Plain, showing the major physiographic features of that area, and distribution of Quaternary alluvium, and Tertiary and Cretaceous sediments.
2. Late Quaternary alluvial deposits in the St. Francis and Western Lowlands Basins (from Saucier, 1974).
3. Idealized field loading conditions (from Seed and Idriss, 1971).
4. Schematic depiction of the location of the zone of liquefaction during earthquake loading (from Seed and Idriss, 1971).
5. Chart for evaluation of liquefaction potential for different magnitude earthquakes (from Seed and others, 1983).
6. Correlation between field liquefaction behavior of sands (average diameter > 0.25 mm) under level ground conditions and modified penetration resistance (from Seed and Idriss, 1981).
7. Distribution of sand boil deposits in Wisconsinan-age alluvium, presumably produced by 1811-12 earthquakes.
8. Energy release center line for the December 16, 1811 earthquake.
9. Modified Mercalli Intensities for the December 16, 1811 earthquake (from Nuttli, 1981).

10. Peak horizontal acceleration in bedrock (average of two components as a function of epicentral distance and body-wave magnitude (m_b) for the central United States (from Nuttli and Herrmann, 1981); and range of possible peak horizontal accelerations in alluvium.
11. Maximum distance from epicenter of liquefaction in sand, as a function of earthquake magnitude (part of this figure is modified from Keefer, in press).
12. Maximum distance from fault-rupture zone of liquefaction in sand, as a function of earthquake magnitude (part of this figure is modified from Keefer, in press).
13. Hypothetical regional intensity map for an 1811-size earthquake having an epicenter anywhere along the New Madrid seismic zone (from Hopper and others, 1983).
14. Modified Mercalli intensity attenuation curves for the central United States (from Nuttli, 1981).

List of Tables

1. Ground slope and expected failure mode of coarse-grained deposits liquefied during earthquakes (after Youd, 1978).
2. Modified penetration resistance values in selected settings in Western Lowlands and St. Francis Basins.
3. Field boring log data at selected locations in Western Lowlands and St. Francis Basins.
4. Central Mississippi Valley historical earthquakes with body-wave magnitudes (m_b) greater than 5.2, exclusive of 1811-12 earthquakes: locations, intensities, and liquefaction.
5. Suggested peak horizontal accelerations as a function of MM intensity for New Madrid earthquake region earthquakes with surface-wave magnitudes (M_s) ≥ 7.0 .
6. Suggested peak horizontal accelerations as a function of MM intensity, for New Madrid region earthquakes with surface-wave magnitudes (M_s) ≤ 6.9 . Data from Krinitzsky and Marcuson (1983).

Earthquake Magnitude Scales

The table below shows equivalent earthquakes for the central Mississippi Valley in terms of Richter local magnitude (M_L), body-wave magnitude (m_b), and surface-wave magnitude (M_s). Data are from Nuttli and Herrmann (1982).

M_L	m_b	M_s
5.0	5.0	4.4
5.2	5.2	4.8
5.4	5.4	5.2
5.6	5.6	5.6
5.8	5.8	6.0
6.0	6.0	6.4
6.2	6.2	6.8
6.4	6.4	7.2
6.6	6.6	7.6
6.8	6.8	8.0
7.0	7.0	8.4
7.2	7.2	8.7

Liquefaction Potential in the Central Mississippi Valley

I Introduction

Both historical accounts of the 1811-12 New Madrid earthquakes and present day evidence show that liquefaction-induced ground failure was very commonplace and widespread in alluvial lowlands, especially between the towns of New Madrid, Missouri, and Marked Tree, Arkansas (fig. 1). This ground failure was typically manifested by sand boils, "earth lurches", ground fissures, and localized distortion and warping of the ground surface. Along streams and in some uplands, many rapid earth flows were doubtlessly caused by liquefaction. If the 1811-12 earthquakes were to recur today, liquefaction-induced ground failure would make impassable much of the Interstate highway system in the St. Francis Basin (fig. 2) from Cairo, Illinois, to nearly as far south as Memphis, Tennessee. Many of the bridges would be knocked down or badly damaged by lateral spreading or collapse of the stream banks. The pavement would be so damaged by ground fissures and warping that it would be impassable at many places, even to 4-wheel drive vehicles. In addition, there might be widespread flooding (Saucier, 1977) due to expulsion to the ground surface of liquefied sand and water. Many houses and other structures would be destroyed by these same causes.

Recounting what took place in 1811-12 and what would take place today given recurrence of such strong earthquakes makes it clear that liquefaction would be responsible for much of the total damage. In what is probably a reasonably analogous situation, the Alaskan earthquake of 1964, liquefaction-induced ground failure caused more than half the economic losses (Mosaic, 1979).

Given the possibility of such dire consequences, exactly where and under what circumstances can liquefaction-induced ground failure be anticipated? Liquefaction generally takes place only in unconsolidated sands or silts, but not all sands or silts have even approximately the same susceptibility. Other important factors are earthquake magnitude and ground response characteristics. It is the purpose of this paper to present data and information so that one can evaluate the regional susceptibility of different materials for different strength earthquakes. To do that, the paper is organized as follows: there is a brief review of factors that cause liquefaction and liquefaction-induced ground failure; the effects of the historical earthquakes in the central Mississippi Valley are examined, to see what data can be extracted; there is an examination and discussion of the various methods that can be used to evaluate liquefaction potential; and material properties are presented, for the geographic area (basically the alluvial area of fig. 1) where there is a moderate to high probability of

liquefaction given recurrence of 1811-12 strength earthquakes. In this way, one can select the method for assessing liquefaction that is best suited for the situation at hand, and make a regional assessment for any earthquake strength.

The paper is written in a format intended to be understandable to geologists, seismologists, and engineers. This necessarily requires some replication of information that is common knowledge within each of these professions. Where words having different meanings within the different professions are possible, such as for the word 'soil', it is the commonly accepted engineering interpretation that is intended. Important words are defined in the text.

Different earthquake magnitude scales are used in the text. Equivalent values for the different scales are in the table after the List of Figures.

II Overview of Liquefaction

Liquefaction is defined as "the transformation of a granular material from a solid state into a liquefied state as a consequence of increased pore-water pressures" (Youd, 1973). In the liquefied state, the material basically behaves as a fluid mass. The increased pore pressure is understood as being caused either directly or indirectly by earthquake shaking (that is, either during or immediately after the earthquake) in this discussion.

A. Conditions for liquefaction

Pore-water pressure buildup in saturated cohesionless soils is caused by the application of cyclic shear stresses induced by ground motions (Seed, 1979). These stresses are generally due primarily to the upward propagation of shear waves. A soil element on level ground undergoes loading conditions as depicted in figure 3, the shear stress applications being somewhat random but nonetheless cyclic. Because of the shearing, cohesionless soils that are sufficiently loose tend to become more compact (that is, occupy less volume). This causes an increase in the pore-water pressure and a decrease in intergranular stress. With continued application of cyclic shear stresses, the pore pressure of loose sands can approach a value equal to the static confining pressure, even though the shear strains are still small. Further cyclic shearing can cause the pore pressure to increase suddenly to the confining pressure, causing large shear straining (even flowage).

Moderately densely packed cohesionless materials ^{1/}, while not nearly as susceptible to large shear straining as loose materials, may still develop a residual pore pressure equal to the confining pressure and cause liquefaction after earthquake shaking. After the cyclic stress applications stop, this

^{1/} Hereafter, moderately densely packed and densely packed materials will be referred to as 'moderately dense' and 'dense', respectively. These density values are relative to one another, rather than absolute values.

residual pore pressure generally causes an upward flow of water. It is likely that the upward flow of water to the ground surface from an underlying layer having a high pore water pressure is the major causative factor in carrying sand to the ground surface and causing "sand blows" (Housner, 1958) or "sand boils" (Seed, 1979).

Liquefaction during earthquake shaking commonly originates in a zone from 2 to 5 m below the ground surface, but can originate at a depth greater than 20 m (Seed, 1979). Generally, the water table must also be near (say, within 3 to 5 m) the ground surface for there to be very serious problems. Figure 4 illustrates that the zone of liquefaction depends on the relationship between the cyclic shear stresses generated by the earthquake and the resistance to liquefaction of the soil.

Seismological factors of prime importance that control liquefaction during shaking include the intensity of the cyclic shear stresses and the number of applications of the shear stresses (Seed, 1979). In the field this translates to shaking intensity (that is, peak acceleration) and duration of shaking. Analytical engineering methods for handling variable cyclic shear stress applications and irregular cyclic stress applications typical of real earthquakes are presently well developed and yield quite acceptable results (Seed and others, 1983), providing the stress histories are known or can be predicted with reasonable accuracy.

B. Materials prone to liquefaction

In areas strongly shaken by the 1811-12 earthquakes, the most common materials prone to liquefaction are sands. Loose clean sands are the most common and widespread susceptible materials, although gravelly sands and silty very fine sands can also liquefy. There are numerous (hundreds) of river and creek depositional terraces in the area of figure 1 which have high water tables and loose sands.

Clean silts with only very small amounts of clay and low cohesion are also susceptible to liquefaction, although probably not to the extent of clean sands. Thick, clean silts, deposited as loess, are commonplace in many upland areas near major streams which carried meltwaters from glaciers. Alluvial lowlands adjacent to loess-covered uplands have a rather thick veneer of soft silt at many places, which originated as loess and was subsequently eroded and redeposited.

Some of the silts in the glacial meltwaters were carried into large bodies of quiet-water, which were lakes in effect, and the silts were laid down in the lake bottoms. There are vast, thick glacial lake deposits north and northeast of Cairo, Illinois. Many of these old lakes presently have high ground-water tables, and the silts are so clean and soft as to be susceptible to liquefaction. Beneath the silts in these old lake beds, there are very loose sands at many places.

Some clay-bearing soils may also liquefy in the event of a New Madrid-strength earthquake. The clayey soils that may be prone appear to be those with less than 15 percent finer than 0.005 mm, a liquid limit less than 35 ^{1/}, and a water content ^{1/} nearly equal to or greater than the liquid limit (Seed and others, 1983). Almost without exception, the only soils with these properties are the silt-rich soils just discussed, and very young sediments in modern flood plains or in very wet swampy areas.

It is also probable that clay-rich sediments which are very young (no older than a few tens or hundreds of years, and very soft (so soft that the sediments are mud), are prone to liquefaction. Soft sediment deformation features, in the class of 'convolute structures', are present in Holocene-age, highly plastic clay strata near Marked Tree, Arkansas. The convolute structures were possibly induced by earthquake shaking. For practical engineering purposes, though, liquefaction is potentially a problem only when clay-rich soils are very soft.

C. Consequences of liquefaction

Liquefaction leads to three basic types of ground failure (Seed, 1968): flow landslides, landslides with limited movement

^{1/} The liquid limit is the water content at which a remolded sample has a soft consistency; the liquid limit is the state at which the sample is on the semisolid-liquid boundary. Liquid limit is measured in a standardized test described in any elementary soil mechanics text. Water content is the ratio, (weight of water)/(weight of dry soil), in percent.

(lateral spreads), and quick-condition failures. In addition, ejection of soil (as by sand boils), and differential loosening and densifying of soil causes differential settling of the ground surface.

For sands, Youd (1978) has suggested that the type of ground failure induced by liquefaction is related to the ground surface slope, and proposed the relationships between ground slope and failure mode shown in Table 1.

The thickness and setting (factors such as depth, lateral continuity, and so forth) of the sand deposit also needs to be considered in determining the probable mode of ground failure. For example, a thin, loose sand layer at a depth of 10 m in an otherwise non-liquefiable clay deposit is not likely to cause a flow landslide or a significant bearing capacity failure, irrespective of the ground surface slope. However, this condition might lead to a translational landslide in steep slopes or magnify ground surface movement due to lateral spreading in flat areas (Anderson and others, 1982).

Flow landslides - On slopes, liquefaction in sands and silts can lead to flows that travel long distances of up to hundreds of meters (for example, see figs. 20-22, Youd and Hoose, 1978). Large soil masses can move as viscous fluids or blocks of intact materials riding on liquefied flows.

Some of the most destructive flows ever recorded originated in loess on hill slopes in Russia (Keefer, in press). Flows in

clays are generally thought to be restricted to sensitive clays. Most clays lose strength when remolded, but sensitive clays have especially large losses. Sensitive clays were involved in many of the most destructive flow landslides in Anchorage, Alaska, in the 1964 earthquake (Mosaic, 1979).

Lateral-spreading landslides - Wherever conditions are favorable for liquefaction but sands or silts occur at depth or are too dense to flow freely during earthquake shaking, limited flow can take place. Even where sands are loose on slope inclinations as low as 0.5 percent, horizontal displacements can be a few feet to more than 2 m, and leave large open cracks at the surface (Youd, 1978). Generally lateral spreads are in alluvial lowlands along streams, where they form parallel to and then move into the stream valley. Lengths of spreads are commonly longest parallel to the streams. Lengths of 150 to 300 m are not unusual (for example, see Fuller, 1912). Rather large lateral spreads can also develop wherever lateral resistance to movement is reduced by removal of only a few meters of soil. Small scarps and man-made ditches are likely locations. Lateral spreads are often commonplace in alluvium as a result of moderate to strong earthquakes.

Quick-condition failures - Seepage forces caused by upward percolating pore water commonly drastically reduce the strength of granular materials, for minutes to days after earthquake shaking. If the strength is reduced to the point of instability,

this state is known as a "quick condition" (this is the same as "quicksand" to the general public).

Quick condition failures are generally found only in thick sand deposits that extend from below the water table to the ground surface. Loss of bearing capacity is a common type of quick condition failure. Buoyant rise of buried tanks, empty swimming pools and water treatment tanks is another common result. During the 1964 Niigata earthquake in Japan, high-rise apartment buildings had quick condition, bearing capacity failures and rotated so much that people could walk on the previously vertical exterior; embankments also subsided into the weakened sands. Landslides can also take place from this effect.

Differential settlements - Wherever seepage forces carry sand and water to the surface, buildings can be undermined. Vertical displacement of the ground caused by compaction of a subsurface soil layer that has liquified and ejected water can cause differential settling of buildings, and perhaps lead to bearing capacity failures. Though probably not often totally destructive of buildings, differential settling can distort and damage structures.

D. Engineering evaluation of liquefaction potential.

Conceptually, various field methods can be used for regional evaluation of liquefaction potential. Recently developed methods include the electrical cone penetration test, the cross-hole seismic velocity test, and pressuremeter test (Youd and Bennett,

1983). These methods are still somewhat experimental in this writer's opinion, and in addition there are so few data for these test methods in the central Mississippi Valley that it is not reasonable to consider using them for regional evaluation. Laboratory dynamic test data on sands are virtually non-existent for the central Mississippi Valley, and it would be prohibitively expensive to develop a reasonable data base using dynamic laboratory testing. The only method for which there are abundant data is the Standard Penetration Test.

Regional evaluation of the liquefaction potential of sand deposits is most commonly done in the field, by testing the soil in-place with the Standard Penetration Test (SPT) blow count method (American Society for Testing and Materials, 1978). A sampling tube is driven into the ground by dropping a 140-lb (63.5 kg) weight from a height of 30 inches (176.2 cm). The penetration resistance is reported in number of blows of the weight required to drive the sampler 1 foot (30.5 cm). The SPT blow counts (N values) are then used in conjunction with anticipated earthquake-induced shear stresses (a function of accelerations) and number of repetitions of the shear stress (related to earthquake magnitude) to determine if liquefaction may take place. Figure 5 shows boundary curves (by Seed and others, 1983) which define where liquefaction is likely to occur for earthquakes with different magnitudes. The figure applies to clean sands with almost no silt, on level ground. (Figure 5 can

be modified for use with silty sands and clean silts that plot below the A-line on the Unified System plasticity chart (Seed and others, 1983, p. 479) by adding 7.5 to the N_1 value before entering the chart). For a given magnitude, data points below or to the right of the curve will almost certainly not liquefy, and data points above or to the left of the curve have a high probability of liquefying sufficiently to cause sand boils (and landslides and other liquefaction-related ground failure). The curves were developed from studies of earthquake-induced liquefaction at many sites around the world.

The field cyclic stress ratio of figure 5 is the ratio, on an element in the sand layer of the average earthquake-induced horizontal cyclic shear stress ($\tau_{h \text{ avg}}$) to the vertical effective stress (σ_{o1}) before the cyclic stresses were applied.

The cyclic stress ratio developed in the field due to earthquake shaking is computed from equation (1) (Seed and others, 1983):

$$(1) \quad \frac{\tau_{h \text{ avg}}}{\sigma_{o1}} = 0.65 \left(\frac{A_{\text{max}}}{g} \cdot \frac{\sigma_o}{\sigma_{o1}} \cdot r_d \right)$$

where A_{max} = peak horizontal acceleration at the ground surface; σ_o = total overburden pressure (weight) on the sand under consideration; σ_{o1} = initial effective overburden pressure (total weight minus water pressure) on the sand layer under consideration; r_d = stress reduction factor ranging from a value of 1 at the ground surface to a value near 0.9 at a depth of about 10 m ; and g = the acceleration of gravity.

For one of the most common field conditions on the terraces and flood plains in the New Madrid earthquake region, where the water table is about 2 m below the ground surface, and the weakest sands are at a depth of 4 to 5 m, the field cyclic stress ratio is almost exactly equal to the peak horizontal acceleration; that is, if the peak horizontal acceleration is 0.20g, the cyclic stress ratio is essentially 0.20.

On figure 5, the modified penetration resistance, N_1 , is the SPT blow count value measured in the field multiplied by a correction factor that accounts for the influence of field stress conditions on the measured blow count; for the field conditions discussed in the paragraph above, the multiplication factor is 1.4 (see Seed and others, 1983).

To illustrate use of the curves, let it be assumed that the peak horizontal acceleration at the ground surface is 0.20g for an earthquake magnitude (M) of $6\frac{3}{4}$, and the SPT blow count in clean sand is 10 (corrected to $N_1 = 14$) on a nearly level terrace for the depth and water table conditions above. These conditions are given by point A on figure 5; liquefaction and production of sand boil deposits would be very probable.

The accelerations required for liquefaction using figure 5 are both a lower bound, and a most probable bound. Figure 6 shows the curve for M equal to $7\frac{1}{2}$, with field data from many earthquakes around the world. The solid circles in figure 6 are for sites where there was evidence of liquefaction-induced ground

failure, such as sand boils. No evidence was observed for open circles; that does not mean that liquefaction did not take place. For example, an especially thick fine-grained cap above liquefied sands prevented sand boils from reaching the ground surface at many places in the St. Francis Basin during the 1811-12 earthquakes (Saucier, 1977; Obermeier, unpublished data). As another example, especially coarse, permeable deposits above the zone liquefied during shaking may dissipate pore pressure so fast that sand boils do not develop. The data in figure 6 are for all types of field settings, and it is not surprising that no liquefaction-related features were observed in some. In summary, it must be concluded that the solid line in figure 6 is probably quite a good bound for estimating accelerations, providing attention is given to the field setting; and, it is extremely unlikely that there would not be liquefaction at accelerations 25 percent higher than the solid line bound.

As noted previously, figure 5 is strictly applicable only for level or nearly level ground. On steeper slopes, higher accelerations are required to cause liquefaction, and more sophisticated methods are used to determine if liquefaction may develop. Still, use of figure 5 helps assess if there is the possibility of problems on the slopes.

The procedure sketched above, known as the "simplified procedure" of Seed and Idriss (1971) indicates only where liquefaction is probable. Disastrous ground failure may or may

not result from an occurrence of liquefaction. In general, liquefied loose sands are much more likely to flow, move large distances, or cause disasters than medium dense sands, even though both sands may liquefy; more rigorous methods are necessary for evaluating the complete scenario.

For clay-bearing soils that plot above the A-line on the Unified System plasticity chart (Seed and others, 1983, p. 479), there are no charts analogous to figure 5. Laboratory test methods must be used at the present time to appraise their behavior in any detail. However, it is certain that serious liquefaction can take place in these materials only whenever they are quite soft. The softness of silts and clays can also be estimated by the SPT method. Only very weak clay-bearing soils that have index and physical properties (natural water content, liquid limit, percent clay) in the range discussed on page 7 are candidates for liquefaction.

III Liquefaction and Historical Earthquakes

Historical earthquakes in the central Mississippi Valley are examined to see what relations can be established between liquefaction, earthquake magnitudes, accelerations, and Modified Mercalli (MM) intensities. Liquefaction effects of the 1811-12 earthquakes are reviewed first, followed by accounts of post 1811-12 earthquakes having body-wave magnitudes (m_b) greater than 5.3.

A. 1811-12 earthquakes

It is well known (Fuller, 1912) that liquefaction-induced ground failure (hereafter called 'liquefaction') took place at

many places many tens of kilometers from the probable epicenters, and locally as far as 175 km (Keefer, in press). Accounts of the farthest liquefaction typically describe disappearing islands in rivers, sand boil deposits near streams, and lateral spreads along stream banks. Almost certainly most if not all of these liquefaction features were in very young alluvial sediments. In general, the youngest sediments are most susceptible to liquefaction, other things being equal (Youd and Perkins, 1978), but the stream energy of the depositional environment can be another important variable, with the highest relative densities being from the highest energy flow regimes (Bennett and others, 1981). The Holocene sediments are from a variety of flow regimes and, in addition, range in thickness from a feather-edge to many tens of meters. This large variation in physical properties and thicknesses causes wide variations in ground response characteristics. Thus, using the regional pattern of liquefaction features to understand earthquake characteristics must be approached very carefully, and would be extremely difficult in a highly variable geologic setting. However, the thickness and physical properties of Wisconsinan-age alluvium in the St. Francis and Western Lowlands Basins presents an almost ideal setting.

1. Alluvium in St. Francis and Western Lowlands Basins

Figure 2 shows alluvial deposits in the St. Francis and Western Lowlands Basins. Almost all the deposits shown in the

eastern two-thirds of the figure are Late Quaternary in age; only locally, generally on modern flood plains, is there other significant alluvium. Total thickness of alluvium is typically between 30 and 50 m throughout the St. Francis Basin (Saucier, 1964), and is only slightly less in the Western Lowlands (Smith and Saucier, 1971). For such thick alluvium, small variations in thickness can cause only minor changes in ground response to an earthquake, providing the physical properties of the alluvium are relatively uniform.

Alluvium of the Western Lowlands and alluvium between the towns of Cairo and Marked Tree is mostly braided stream terraces of glacial outwash or valley train deposits. These terraces are typically a layered sequence of 'topstratum' over 'bottomstratum' (Saucier, 1964). The topstratum is generally a 2 to 6 m thick overbank deposit, which contains thick to thin strata that are very clay-rich, highly plastic, and black; the topstratum has greatly subordinate strata of silt and very fine sand. The topstratum texture abruptly grades down into the bottomstratum, over a distance typically less than a meter. The bottomstratum is very clean, moderately dense sand, which is generally fine- to medium-grained near the top, and grades downward to a coarse sand with gravel at the base.

Meander belt deposits laid down by the Mississippi River generally have thick strata of clean sand, silty fine sand, and clay within the uppermost 10 to 15 m. Beneath that are clean

sands. There is a clay-rich cap of overbank deposits over these meander belt deposits at many places, especially in lower elevation places. The total thickness of clay rarely exceeds 10 m. Within these meander belts, there are usually many places nearby where the clay cap is only a few meters thick, and clean sand underlies the cap. Overall, braided stream and meander belt deposits are almost certainly the same with respect to seismic response characteristics.

2. Sand boil deposits in St. Francis Basin

Figure 7 shows the distribution and density of areal coverage of sand boil deposits in the Wisconsinan-age alluvium of figure 2. Figure 7 is based on an investigation by the author, using 1938-1940 vintage and more recent airphotos (scale about 1:20,000) in conjunction with extensive field verification. Field verification was required because other features visible on airphotos such as sand dunes and mima mounds ^{1/} look similar to sand blow deposits. The older photos were used because in recent years large tracts of land have been regraded for agricultural uses, obliterating evidence of sand boil deposits.

Field and airphoto studies for figure 7 were restricted to the St. Francis Basin and the eastern one-third to one-half of the Western Lowlands Basin. Some unknown features, possibly sand

^{1/} Mima mounds are small mounds which are dominantly sand, circular in plan view, that are generally from 0.5 to 1m in height, and 5 to 10m in diameter. They are of unknown origin, but are not sand boils caused by the 1811-12 or younger earthquakes.

boil deposits, were found in the Western Lowlands Basin, but appeared to be too weathered to be associated with 1811-12 earthquakes. All sand boil deposits in the St. Francis Basin appeared unweathered or only slightly weathered, and thus were attributed to the 1811-12 quakes.

Much of the field and airphoto effort was directed to locating the margin of liquefaction effects, which was empirically defined as the outer limit where at least three percent of the ground surface is covered by sand boil deposits (smaller percents are difficult to determine from airphotos). In that way, the location of the 'energy release center' could be estimated for the December 16, 1811 earthquake, and earthquake accelerations could be estimated away from near-field effects, using the relations in figure 5.

3. Energy release center

Based on regional earthquake intensity studies, Nuttli (1979) estimated the three large 1811-12 earthquakes had the epicenters shown on figure 8. Although the epicenters are very approximate, it is likely that the first strong quake, the December 16 event, was located considerably southwest of the other two. Thus, it seems reasonable to associate the southernmost one-third of sand boil deposits with the December 16 event. Nuttli's estimated epicenters for the other two large events are so close to one another that use of the pattern of sand boil deposits to locate energy release centers would be

extremely difficult, if not impossible.

A cursory examination of figure 7 suggests that the energy release center for the December 16 quake is a line centrally located to the boundary of sand boil deposits, roughly in the southern one-third of these deposits. In addition, the line trends southwest-northeast, and has a southern terminus that is a little north of Marked Tree (see fig. 8). This energy center line location is based on the premise that the Wisconsin-age alluvium in the region has about the same liquefaction potential.

The writer investigated the physical settings and engineering properties of alluvium in the St. Francis and Western Lowlands Basins by compiling some 400 boring logs. Most of the data were collected from files of the Army Corps of Engineers, Memphis District. About 250 of these had SPT data to a depth of about 12 to 15 m. The borings were scattered throughout the area, but most were near levees or large drainage ditches excavated throughout the basins. Data from very young alluvium along small streams was excluded. To fill in some voids in the data, the writer conducted 30 more SPT borings.

The data were separated according to the following geographic-geologic settings: braided stream terraces, Western Lowlands Basin; southern half of braided stream terraces, St. Francis Basin; and Mississippi River meander belt deposits. The southern half of braided stream terraces in the St. Francis Basin was further subdivided into four large areas. It was found that

in meander belt deposits, layers of silty very fine sand and very fine sand are much more commonplace than in braided stream terrace deposits, which generally have much coarser sands. This textural difference required making a correction to the N_1 value (the method of Tokimatsu and Yoshimi (1981) was used) to account for the influence of grain size on liquefaction potential. It was also found there are no substantive differences in SPT blow counts or sand textures in braided stream deposits, throughout the southern part of the St. Francis Basin.

Table 2 shows results of the study. The table shows 'modified penetration resistance' (N_1) values, which is the field SPT blow count modified to account for the influence of overburden pressure and water table location. N_1 is the value used in the 'simplified procedure' of Seed and Idriss (1971) (see fig. 5). The N_1 values are for the depth range generally most susceptible to liquefaction, 3 to 8 m. Median and lower quartile (i.e., the 25 percent) values are given because they are thought by the writer to realistically bracket what percentage of a sand body must be liquefied to form sand boil deposits, in this depth range. Requiring that half the volume of sand liquefy is a severe requirement, because liquefaction of a single, loose layer can be adequate for production of extensive sand boil deposits. For a significant regional development of sand blow deposits, though, there must be some significant degree of liquefaction, although the lower cut-off is very uncertain and must depend on

factors other than N_1 (such as the topstratum thickness or the rate at which the excess pore water pressure can be dissipated in strata overlying the layer liquefied during shaking).

Irrespective of whether the median or lower quartile is more appropriate, table 2 shows that in the St. Francis Basin, N_1 values are basically the same in braided stream terrace deposits and Mississippi River meander belt deposits, and both types of St. Francis Basin alluvium have higher N_1 values than Western Lowland braided stream terrace alluvium. The topstratum is so thin at many places (less than 3 to 4 m) in both the Western Lowlands and St. Francis Basins that an excessive topstratum thickness could not have been a major factor in determination of the outer bound of sand boil deposits, at least regionally. Thus, the energy center for the December 16, 1811 should lie approximately in the center of the outer limits of sand blow deposits. From this knowledge, the southern limit and orientation of the energy release center shown on figure 8 was established; the length of the energy release center line was determined using an estimate of the length of rupture, reported by Nuttli (1983).

Consideration of the pattern of sand boil deposits (this paper), the modern seismicity (Stauder, 1982), the in-place stress field in lithified rocks (Hamilton and Zoback, and the overall style of surface deformation (Russ, 1982), strongly suggest that the December 16 earthquake was strike-slip, and parallel to and very close to the line of energy release on

figure 8.

4. Accelerations in alluvium

Sites generally best suited for back-calculating earthquake accelerations are outer margin locations of sand boil deposits, where liquefaction can cause only minor changes in pre- and post-earthquake SPT data. No data were available along the margin, but 10 STP borings were at scattered sites beyond the margin, where no sand boils were observed. Thus, at these sites, earthquake accelerations determined using the smallest N_1 values are maximum possible accelerations; actual values were somewhat smaller. It is assumed that the December 16 earthquake had a M_s value of $8\frac{1}{2}$ (Nuttli, 1983).

Three of the borings were between Marked Tree and Memphis, (in the St. Francis Basin); these borings were about 40 km south of the energy center line (see table 3). The smallest N_1 values that were relatively commonplace were about 17 to 20. Using the chart in figure 5 to determine the cyclic stress ratio for a M_s value of $8\frac{1}{2}$, and then calculating the acceleration from equation (1), yields a peak horizontal acceleration of about 0.18g. Two borings in the Western Lowlands (see table 3), 45 and 52 km from the energy center line, yielded peak horizontal accelerations of about 0.19g. Thirty-two km north of the energy center line, the data yielded 0.19g; the borings north of the energy center line were from sites where it was rather difficult to detect sand boil deposits, because of the generally sandy texture of surface

soils, and therefore much less confidence can be associated with these accelerations. However, based on data from south of the energy center line and from the Western Lowlands Basin, it is very probable that at 40 to 45 km from the energy center the peak horizontal accelerations at the ground surface were less than 0.20g.

5. Accelerations in bedrock

The lack of strong motion ground response data for the New Madrid earthquake region makes it difficult if not impossible to relate accelerations in alluvium to bedrock motions, except by empirical relations elsewhere and semi-quantitative calculations. Seed and Idriss (1982, p. 37) have shown that, on average, at 0.20g, the peak acceleration in rock is nearly the same as in soil. Sharma and Kovacs (1980), in a microzonation study of the Memphis area using the program SHAKE, found that peak accelerations in the deep sands (greater than 30 m thick) of the area are about the same as in the underlying bedrock for strong earthquakes in the New Madrid fault zone (which is in about the same place as the energy release center line of figure 8); their data show that peak accelerations in the deep sands should range from about equal to not more than about 15 percent smaller than in the underlying bedrock. All the accelerations back-calculated in the preceeding section were from sites where sand exceeded 30 m in thickness. Thus, it seems quite likely that at those locations the peak accelerations at the ground

surface were about the same or only slightly lower than in the bedrock beneath.

6. Farthest liquefaction

The farthest lateral spreads or flows were about 175 km from the 1811-12 earthquake epicenters, according to Keefer (in press). O. W. Nuttli (St. Louis University, oral communication, 1983) has found historical accounts of sand boil activity in the flood plain of the Mississippi River, near St. Louis, and along the Wabash River. St. Louis is about 250 km from the epicentral region; sand boils in the Wabash River valley were about 300 km from New Madrid. Sand boil deposits on loose, level alluvium should develop further from the epicenter than lateral spreads or flows, so the data by Keefer and Nuttli seem consistent with one another.

B. Other historical earthquakes

Table 4 is a compilation of central Mississippi Valley historical earthquakes having body-wave magnitudes equal to or higher than 5.3, and the associated accounts of liquefaction and Modified Mercalli (MM) intensities. Liquefaction was reported only for the 1895 earthquake (which is also known as the Charleston, Missouri, 1895 earthquake). Sand boils occurred at scattered locations over a region about 16 km in diameter, at places north of Charleston, in Charleston, and south and southwest of Charleston (Powell, 1975). This region where sand boils developed is in braided stream alluvium (see fig. 2) which

is only a little less prone to liquefaction than at other places in the Wisconsin-age alluvium of the Western Lowlands and St. Francis Basins. Thus, it seems reasonable that for braided stream deposits in both basins, the threshold for liquefaction is m_b between 5.5 and 6.0. This assumes that back-calculated magnitudes are reasonably accurate.

C. Earthquake intensity and liquefaction

Table 4 has no reports of liquefaction for MM VII or lower. Alternately, the MM VIII area of 1895 Charleston earthquake had liquefaction in sediments that are moderately dense and at least moderately difficult to liquefy. It seems incongruous that there are no reports in table 3 of liquefaction for the 1895 or any other earthquakes in very loose flood plain deposits for MM VII, and yet liquefaction in moderately dense materials at MM VIII. The writer thinks it is probable that there were sand boils in flood plain alluvium for many of the MM VII quakes, but they were not reported. Sand boils develop in the flood plain behind both natural and artificial levees along the Mississippi River after many of the largest annual floods, and are so commonplace as to not receive special attention.

Figure 9 is a map by Nuttli (1981) showing intensity data for the December 16, 1811 earthquake. Locations of farthest sand boils (in Mississippi River flood plain near St. Louis and the Wabash River valley) are in the zone of MM VII intensity.

Thus, it is concluded that MM VII is the liquefaction threshold for the very loose flood plain sands, irrespective of earthquake magnitude. This conforms to findings by Keefer (in press).

It might seem to follow that MM VIII is the threshold for the moderately dense Wisconsinan-age alluvium in the Western Lowlands and St. Francis Basins, but that does not seem to be true. Comparison of figure 9 with figure 7 shows that the outer bound of sand boils, in the southern third of sand boils deposits, does not extend beyond the boundary for MM X. Part of this discrepancy of MM intensity and liquefaction threshold is probably due to the fact that the MM intensity scale is often a very poor measure of earthquake acceleration even for a given earthquake.

IV Critique of Historical and Other Data

The acceleration, magnitude, and intensity data and their associations with liquefaction, reported in the previous section, are further evaluated and compared with data from other sources to determine the most reasonable approach for evaluating liquefaction potential.

A. Accelerations

The peak horizontal acceleration in bedrock for the December 16 earthquake, previously determined near the margin of sand boil deposits, was probably about 0.20g at 40 to 50 km from the southern terminus of energy release center. Figure 10 is a plot

by Nuttli and Herrmann (1981) showing the peak horizontal acceleration (average of two components) as a function of epicentral distance and body-wave magnitude for the central United States. Nuttli and Herrmann do not specify the material, but it is presumed to be bedrock at higher accelerations. It is not possible to make direct comparisons of acceleration between figure 10 and the epicenter and energy release center line for the December 16 earthquake, because the energy released may have varied along the fault, and because the epicenter may not have coincided with the zone of maximum energy release. However, for discussion purposes, it is assumed that the epicenter was coincident with the zone of maximum energy release (which is the matter of major concern for this study of liquefaction). With this constraint on the epicenter, some bounds can be placed on acceleration as a function of distance from the epicenter.

The classical definition of epicenter is the point on the earth's surface directly above the earthquake focus (the focus is the point at which strain energy is first converted to elastic wave energy). Thus, the epicenter may or may not be coincident with the point of maximum energy release. Although Nuttli and Herrmann do not state so in their text, their usage also implies that their epicenter is coincident with the point of zone of maximum energy release.

Assuming that the energy released was uniformly distributed along the energy release line would yield a peak horizontal

acceleration of 0.20g about 40 km from the epicenter. This is shown as point A in figure 10. Point A is almost certainly a lower bound of acceleration at this distance from the epicenter. The farthest northward location of an epicenter that is possibly associated with the pattern of sand boils is the northern end of the energy release line; if the epicenter was further north there should have been widespread liquefaction further northwest of New Madrid, in the braided stream deposits between Sikeston Ridge and Crowleys Ridge (fig. 2). Thus, as a maximum, the peak horizontal acceleration was 0.20g at 110 km from the epicenter, along the axis of the energy release line. This is shown as point B on figure 10. This upper bound includes the maximum possible effects of focusing along a strike-slip fault. Point B is the point which the writer considers as the absurd upper limit. Almost certainly the northern limits of sand boils were the result of the February 7, 1812 earthquake, which probably had its epicenter near New Madrid (Nuttli, 1979; Obermeier, unpublished data). Acceleration data based on locations of sand boil deposits seem somewhat lower than the curve for m_b equal to 7.3. A value of m_b equal to 7.2 is equivalent to M_s of 8.7 (M_s for the December 16 earthquake is presumed to be about $8\frac{1}{2}$). Thus, the curve by Nuttli and Herrmann indicates somewhat higher accelerations than the liquefaction-based data. It should be also noted that the Nuttli-Herrmann relations on figure 10 are the average of two

components. Liquefaction, however, is controlled primarily by the peak component of acceleration (Seed and others, 1975). This again makes the Nuttli-Herrmann values seem too high.

The 1895 Charleston earthquake liquefaction data also indicate that the Nuttli-Herrmann accelerations are too high. The diameter over which there were scattered sand boils in braided stream alluvium did not exceed 16 km. For an m_b value of 6.2 (table 2), figure 10 shows that the peak accelerations should have been basically independent of distance from the epicenter for 20 km; thus, the diameter of sand boil deposits should have been at least 40 km, which far exceeded field observations. The standard error of estimate for the Nuttli-Herrmann curves on figure 10 is about 2 (Nuttli and Herrmann, 1978), which is quite large. (The possible sources of error are noted in a paper by Krinitzsky and Marcuson (1983)). Nuttli (oral communication, 1983) has expressed to the writer, however, that whereas the acceleration values may have a large error, the attenuation relations are quite realistic.

The most reasonable epicenter for the December 16 earthquake is the center of the southernmost large area of very intense sand boil development, shown on figure 8. Throughout much of this large area the volume of liquefied sand was so great at most places as to make a continuous sheet of sand, 1 to 1.5 m thick. North of this area of the sand sheet, and northeast of the point showing Nuttli's December 16 epicenter, there are only localized

places where the sheet of sand is continuous. This 'most reasonable epicenter' is shown as point C on figure 10.

The writer believes that the most reasonable curve of acceleration as a function of epicentral distance, for m_b equal to 7.1 (equivalent to M_s of 8.5), goes through point C and is parallel to the curves for m_b equal to 7.3 and 6.5. It should be a relatively simple matter to adjust the curves for other values of m_b , by consulting papers by Nuttli and Herrmann (1978; 1981). Then, using the adjusted curves to determine the acceleration for the magnitude and epicentral distance in question, and adjusting the accelerations for local seismic response conditions that may affect the values (such as thickness of alluvium and dynamic modulus properties), the liquefaction potential can be assessed from figure 5. This assessment would be for movement along a strike-slip fault, along the axis of the fault, and thus would be an upper limit of reasonable assessments.

Also shown on figure 10 is a data point (C^1) that represents the upper bound of reasonable peak horizontal accelerations in bedrock at distance C from the epicenter. This upper bound is based on the premise that the accelerations based on figure 5 may be as much as 25 percent too low, and that peak accelerations in the sand may have been 15 percent lower than the underlying rock. The acceleration at C^1 is 0.29g.

B. Magnitudes

Both theoretical approaches (Youd and Perkins, 1978) and field observations of liquefaction features (Kuribayashi and Tatsuoka, 1975; Youd, 1977; Youd and Perkins, 1978; Davis and Berrill, 1983; Keefer, in press) demonstrate that there is a reasonably well-defined relationship between the farthest extent of significant liquefaction and distance from the epicenter, for different magnitude earthquakes and a fixed susceptibility to liquefaction. The field observations were predominantly in Holocene-age silt, silty sand, or sand. These materials typically have moderate to high susceptibility to liquefaction (Youd and Perkins, 1978).

Figure 11 shows results based on field observations from around the world, and some suggested practical bounds on the limits of localized damaging liquefaction. The solid line is the outer limit of lateral spreads or flows, based on data by Davis and Berrill (1983) and by Keefer ^{1/} (in press) from more than 46 earthquakes, scattered around the world. Very probably, most

^{1/} Smallest displacements reported in the paper by Keefer are at least 40 mm; however, at least some very few data points that Keefer shows in his figures could have had smaller displacements (Keefer, personal communication, 1984). For these reasons, it is presumed that for practical purposes the lateral displacements were greater than 40 mm.

In his original compilation, Keefer used moment magnitudes (M_w) for M values greater than 7.5; a replot of Keefer's data for figures 11 and 12 using surface wave magnitudes (M_s) shows basically no change in the curve of outer limit of reported data. Values of M_s for the replot of the 1811-12 earthquakes are from Nuttli (1983).

of these data are from sites where there was greater than 40 mm of differential vertical or lateral movement, which should be adequate to damage only poorly built masonry structures. The dashed line is the best fit of data for all types of liquefaction-induced ground failure in Japan, including sand boils, reported by Kuribayashi and Tatsuoka (1975). The dotted line is the outer limit on natural deposits from all data sources, for practical purposes. (Keefer's compilation includes both natural deposits and artificial fill.). The figure also shows that the farthest liquefaction from the 1811-12 earthquake epicenters did not extend an unusually large distance, compared to other earthquakes. This seems surprising at first, because of the huge area over which the 1811-12 earthquakes caused high MM intensities. It is possible that occurrences of sand boils and other liquefaction-features took place much further than some 250 km from the epicenter and was not observed, but the writer does not believe that to be the case. In 1811, there were many settlers in western Kentucky and along the Ohio River valley, which has a wide flood plain westward from the mid-longitude of Indiana. This flood plain contains thick deposits of clean sand at many places. Natural levees along the Ohio River are generally small features and not very high, and sand boils caused by flooding are not commonplace. Surely, because they are unusual, sand boils caused by the 1811-12 earthquakes would have been noticed and reported. Instead, it is more likely that the

alluvium in these flood plains is not as loose as at many of the other localities with liquefaction in figure 11. Probably, only river channel and very young point bar deposits in the central Mississippi Valley region have very high susceptibility, and these would be the only materials liquified at the limits of the dotted line in figure 11.

Figure 11 also shows a conservative, yet not extremely conservative, outer limit for marginal liquefaction for braided stream terrace and Mississippi River meander belt deposits in the St. Francis Basin shown on figure 2. These limits were determined by using point C on figure 10 as the maximum distance from the epicenter to liquefaction features for the December 16 earthquake (this is believed by the writer to be conservative because it is the distance from the center of high intensity sand boil development to the farthest southwestern boundary of sand boils). The distance from the center to the edge of sand boil deposits near Charleston is used as distance from the epicenter for the 1895 earthquake. The data from historical earthquakes in table 3 provide a third point at M equal to 5.0. The shape of the curve has also been chosen to be conservative. For magnitudes less than 7.8 and larger than 6.8, the slope is the same as for much weaker sands; the overall shape conforms to that of the outer limit (solid) line. This curve for St. Francis Basin deposits, at the limits of marginal liquefaction, probably represents the outer limits where there would be some serious

structural damage to poorly built, old, commercial or residential brick or block buildings, but well-built masonry buildings and houses would only be cracked.

As pointed out by Youd and Perkins (1978) epicentral distance is not a very good measure for the type of correlation in figure 11, because the epicenter does not define the entire zone of energy release, particularly for large earthquakes. They suggested, therefore, that the seismic source zone is a better point of reference. Keefer (in press) has prepared a plot showing the maximum distance of lateral spreads and flows from the fault-rupture zone, and that plot is the primary basis for figure 12. Figure 12 shows the following: for practical purposes the outer limit (solid line) for lateral spreads or flows with greater than 40 mm of movement in predominantly loose sediments; the outer limit (from Youd and Perkins, 1978) for greater than 100 mm of movement in predominantly loose sediments; and the practical outer limit for marginal liquefaction in St. Francis Basin alluvium in figure 2, exclusive of very young alluvium along the Mississippi and other rivers. Youd and Perkins selected 100 mm as the minimum displacement required to cause significant damage to most structures.

Fault rupture locations for the 1811-12 earthquakes were estimated from fault zones on figure 8. For the December 16 earthquake, the fault zone north of Marked Tree was used as the reference point from which to measure the farthest liquefaction,

which was taken to be the outer bound of sand boils southwest of Marked Tree. For the February 7 earthquake, the fault zone at Reelfoot Lake was used as the reference point, and the farthest liquefaction was taken to be northernmost bound of sand boils in the braided stream deposits between Sikeston Ridge and Crowleys Ridge. The fault rupture for the 1895 Charleston earthquake was the location central to the margin of sand boils.

The bound by Youd and Perkins is only slightly closer to the fault-rupture zone than a bound by Kuribayashi and Tatsuoka (see Youd and Perkins, 1978) for the best fit of data to farthest liquefaction from the epicenter. For that reason, and because there are proportionally so few data between the bound by Youd and Perkins (dashed line) and the outer limit of reported data (solid line), it is suggested that the dashed line is a conservative limit for potentially damaging liquefaction in natural loose deposits (median N_1 values of about 10 or less or N_1 values of about 5 or less). The dashed-dotted line is thought reasonable for the alluvium in the St. Francis Basin shown in figure 2, except for very young alluvium along smaller streams and along the Mississippi River. The dashed line should be used for the very young alluvium.

It was noted previously that in figure 12 the slope of the bounding line for braided stream deposits is a conservative estimate. The slope and origin of the bounding line can be calculated for the moderately thick braided stream deposits with

any N_1 value from the equations below.

According to Youd and Perkins (1978), a reasonable relation between τ/σ'_o and earthquake magnitude, M , as a function of distance, r , from the earthquake source is

$$(2) \quad \tau/\sigma'_o = k_1 r^{-k_2} \exp(k_3 M)$$

in which k_1 , k_2 , and k_3 are constants. The curves in figure 5 are of the form

$$(3) \quad \tau/\sigma'_o = k_4 N_1^{(k_5 - k_6 M)}$$

in which k_4 , k_5 , and k_6 are constants. Constants for equation (3) can be determined from the curves in figure 5.

Setting equation (2) equal to equation (3), r can be solved as a function of N_1 . The remaining constants can be bracketed from curves and data in figure 12.

C. Intensities

A weakness with evaluating liquefaction potential by either estimated accelerations from the epicenter (fig. 10) or observations of the distance of liquefaction features from epicenters (fig. 11) or fault ruptures (fig. 12) is that these methods over-estimate the geographic region prone to liquefaction. All these methods show only the farthest limits, accounting for effects of focusing of energy, site amplification or unusual circumstances. Next, consideration will be given to whether MM intensity historical data may help to make more realistic evaluations of regions with potential liquefaction problems.

Intensity data from all the larger historical earthquakes in table 2 with epicenters roughly in the zone of most frequent modern seismic activity (Stauder, 1982), extending from approximately Marked Tree to Cairo, clearly show MM intensity values VII and higher are consistently strongly focused in much the same geographic area. Hopper and others (1983) in a study of the earthquakes in 1811, 1843, and 1895 (listed in table 4), found that the largest MM intensities were in a region oriented approximately parallel to the zone of modern seismicity, and in addition there was some focusing near the Mississippi River, extending from near Cairo toward St. Louis. Figure 13 shows what Hopper and others refer to as a "hypothetical regional intensity map for an 1811-size earthquake having an epicenter anywhere along the New Madrid seismic zone (the zone of current intense microseismicity)". The map was made by drawing MM intensity contour maps for the 1843 and 1895 earthquakes, and then scaling them to the 1811 earthquake. For example, the highest MM intensity for the 1895 earthquake was VIII, and the highest for 1811 was XI; thus a value of III was added to all the 1895 values. This simple additive method places undue importance on accurately establishing MM intensities, especially near the epicenter and in addition implicitly assumes that accelerations vary in much the same manner as other facets of ground movement (i.e., velocity and displacement) that cause damage in earthquakes. Thus, the intensity values are somewhat suspect as measures for liquefaction.

In addition, MM intensities are not a particularly good measure for liquefaction potential because liquefaction is controlled primarily by the number of applications of high shear stress, and thus earthquake magnitude. To circumvent this problem, MM intensities and associated accelerations are suggested first for strong, 1811-12-type earthquakes, and then for weaker earthquakes.

For the December 16, 1811 earthquake, the back-calculated peak horizontal acceleration at the margin of liquefaction in braided stream and Mississippi River meander belt deposits was determined to be about 0.20g, and was probably not greater in the underlying bedrock, and very probably did not exceed 0.25 g in bedrock. The margin of liquefaction is very close to the MM intensity X contour in figure 9.

It is probable that the peak accelerations for the 1811-12 earthquakes, far from the epicenters, did not exceed typical values at other places around the world for about the same magnitude quakes; this is supported by data by Keefer (in press) which show that in 1811-12 the farthest limits of spreads and flows were, if anything, closer to the epicenters than for most other earthquakes of the same magnitude (see fig. 11). Thus, it is believed that correlations by Krinitzsky and Marcuson (1983) between MM intensities and mean values of peak horizontal accelerations for strong earthquakes ($M_s \geq 7.0$) should be conservative values for New Madrid region strong earthquakes.

Krinitzsky and Marcuson do not have data for MM intensities larger than VIII. Their data for strong earthquakes are in table 5, which lists peak horizontal accelerations. Table 5 also includes data from this report, for a MM X intensity.

Because of the paucity of data in the New Madrid region, the relations by Krinitzsky and Marcuson are probably as good as can be suggested for M_s less than 6.9. Their value of 0.20g for the far field, soft site, seems quite reasonable, based on back-calculations of accelerations required to liquefy braided stream deposits in the 1895 Charleston earthquake. Table 6 lists suggested peak horizontal accelerations.

All the data in tables 5 and 6, irrespective of whether from the report by Krinitzsky or Marcuson or this paper, should be considered as mean values of peak accelerations. These values are for non-critical structures. For critical structures, these values should be increased by a factor of about 1.4 to 1.5, based on data and a suggestion by Seed and Idriss (p. 40, 1982).

There remains the question of determination of the proper intensity value for a given earthquake. For an 1811-size earthquake ($M_s \simeq 8\frac{1}{2}$), figure 13 shows MM intensities that approach the highest that could be expected, accounting for unusual amplification of bedrock motions. An alternate approach is to use MM intensity relations in figure 14, by Nuttli and Herrmann (1981). The curves in figure 14 are based, beyond 25 km from the epicenter, on equation (4)

$$(4) \quad I(r) = 0.40 + 2.00 m_{bLg} - 2.70 \log_{10} r - 0.0011 r$$

where r is epicentral distance (in kilometers), I is the MM intensity at distance r , and m_{bLg} is the body-wave magnitude as determined from the amplitudes of 1-Hz Lg waves, which are higher-mode surface waves.

Intensity values based on this equation are somewhat lower and less conservative than figure 13, especially for the northeastern half of figure 13. Intensity values for equation (4) are much closer to anticipated mean values.

V Liquefaction Susceptibility and Geologic Origin

The texture, mode of deposition, and age affect liquefaction potential in a generally predictable way (Youd and Perkins, 1978). Sediments in the central Mississippi Valley can be categorized for liquefaction potential, on a regional basis, based on units on surficial geologic maps. Surficial geologic maps are available in all States at a scale of 1:1,000,000, and in some States at scales which show much more detail. Maps at a scale of 1:62,000 or 1:24,000 are more optimal, but are generally available only for localized areas.

Many of the deposits on the State maps have formation names, which may change at a State boundary. For that reason, names are not used in this discussion, but rather the geologic origin and age are used as a basis. Liquefaction potential is given in terms of median N_1 values whenever possible.

A. Braided stream and meander belt deposits.

The properties of Wisconsinan-age braided stream terraces made up of glacial deposits and Mississippi River meander belt deposits on figure 2 have been described previously in the text and in table 2, and will only be summarized here. Median N_1 values are generally near 25, and there are abundant thick clean sands which fine-upward to a thin stratum of fine or silty sand just beneath a clay-rich cap, 3 to 6 m thick. Glacial deposits having about the same properties are present at many places along many of the larger streams which carried glacial outwash. The Wabash, and Ohio Rivers laid down especially large volumes of clean sand in Illinois and Indiana. Thicknesses of 30 m are not unusual.

Although rivers further south did not carry glacial outwash, many have terraces Late Wisconsinan in age or older, that are dominantly thick clean sands. The Obion River in Tennessee has some especially large terraces. The terrace deposits along the southern rivers probably have about the same resistance to liquefaction as the braided stream deposits in the St. Francis and Western Lowlands Basins, because they are all about the same age and all have minerals with about the same physical properties.

B. Glacial lake deposits.

Large glacial lakes formed along many rivers carrying glacial meltwater, particularly in Indiana, Illinois, and

Kentucky. Many of these glacial lakes laid down thick deposits of sand, silt, and clay. At many places there is a fining-upward tendency from a basal sand. Thicknesses of 15 m are commonplace.

Near large streams, thick and unusually loose sands (N_1 about 8) about 6 m deep are at many places. At most other places the sands are denser and have much higher N_1 values. Very soft silts and clays with SPT blow counts of 2 to 3 are relatively common in lower areas throughout Indiana, Illinois, and Kentucky. The higher, better drained sites typically have much higher blow counts due to effects of dessication and a lower ground water table.

C. Flood plains, exclusive of very young sediments.

Very young sediments are defined as those less than about 500 years old, and are generally point bar deposits or sand bars. Exclusive of these, flood plains along major streams generally have thick strata of clean sand, silt, and clay. The sands generally have median N_1 values of about 20, though locally N_1 values of 15 are commonplace. Silt and clay strata in some abandoned channels are so soft as to be potentially subject to liquefaction.

D. Very young sediments.

The only very young sediments of concern are along streams. Very loose, thick sands are commonplace along larger streams and some smaller streams as point bar deposits or sand bars. N_1 values less than 10 are commonplace.

E. Eolian deposits.

Thick loess deposits are present in upland areas near the major streams that carried large volumes of glacial meltwater.

The Wabash and Mississippi Rivers have especially thick deposits on nearby uplands, especially east of the rivers. Near the rivers, thicknesses of 20 to 25 m are not unusual. The loess is predominantly silt, with almost no cohesion at some places. Even clayey silt loess can have an extremely low cohesion and sensitivity as high as 10, and is potentially subject to liquefaction with large shear straining or flowing (Randall Jibson, U. S. Geological Survey, personal communication, 1984). Locally, and especially near large rivers, loess has lenses of clean, very loose dune sand or water-deposited strata of clean sand. In the highly dissected upland areas with thick loess, the loess may be only locally or partly saturated far beneath the ground surface.

The writer is unaware of any soil mechanics, dynamic laboratory test data on loess in the area. It is probable, though, that where the ground water table is high, slopes in loess are potentially subject to flowing failure during earthquakes.

F. Reworked eolian deposits.

At the base of the high loess bluffs along major rivers, there is generally a veneer of silt washed down from the hills. This veneer is 6 m thick at many places, and in lowland areas is

very soft at many places. Clearly many of these sediments are weak enough to liquefy in moderate to severe shaking, though in most cases liquefaction would be accompanied by only limited straining. To the writer's knowledge, the only data relevant to evaluation of dynamic behavior of reworked eolian materials is in a 1983 Ph. D. thesis by Vijay Puri, of the Missouri School of Mines, Rolla, Missouri.

VI Summation

There are so few data on strong earthquakes that all the methods most commonly used for evaluating liquefaction potential, based on accelerations, magnitudes, or intensities are somewhat suspect. Even a regional assessment should be based on results from more than one method and requires a considerable amount of judgment.

There are many large terraces and flood plains in the central Mississippi Valley region which contain moderately dense to loose clean sands and silty sands. Evaluation of their liquefaction potential is reasonably easy and straightforward, providing the acceleration-magnitude relations are known. However, there are also many thick glacial lake deposits, eolian deposits, and reworked eolian deposits made up of silt-rich materials of highly varying liquefaction potential. Field methods for assessing their properties are extremely crude at best, and there appear to be so few laboratory data that there are no guidelines based on simple criteria such as void ratio,

cohesion, and plasticity characteristics. It should be a relatively simple matter to do such a thing.

The level of earthquake accelerations plays a very important role in liquefaction. The back-calculated accelerations presented in this paper for the 1811 earthquake have some degree of uncertainty, but the writer strongly believes they are accurate within 25 percent. These numbers can be verified, in alluvium, by collecting undisturbed samples (by means of freezing samples in the field), and then testing in the laboratory with a shake-table.

References Cited

1. American Society for Testing and Materials, 1978, Annual book of ASTM standards, pt. 19, Designation D 1586-67 (Reapproved 1974), Standard method for penetration test and split barrel sampling of soils: Philadelphia, Pa., p. 235-237.
2. Anderson, L. R., Keaton, J. R. Aubry, K., and Ellis, S. J., 1982, Liquefaction potential map for Davis County, Utah: Dames and Moore Consulting Engineers, Salt Lake City, Utah, 49 p.
3. Bennett, M. J., Youd, T. L., Harp, E. L., and Wieczorek, G. F., 1981, Subsurface investigation of liquefaction, Imperial Valley Earthquake, California, October 15, 1979: U.S. Geological Survey Open-file report 81-502, 83 p.
4. Coffman, J. J., and von Hake, C. A., 1973, Earthquake history of the United States: U.S. Department of Commerce, National Oceanic and Atmospheric Administration, Publication 41-1, 208 p.
5. Davis, R. O., and Berrill, J. B., 1983, Comparison of a liquefaction theory with field observations: The Institution of Civil Engineers, London, Geotechnique, vol. XXXII, no. 4, p. 455-460.
6. Fuller, M. L., 1912, The New Madrid earthquake: U.S. Geological Survey Bulletin 494, 119 p.

7. Hamilton, R. M., and Zoback, M. D., 1982, Tectonic features of the New Madrid seismic zone from seismic reflection profiles: in McKeown, F. A. and Pakiser, L. C., ed., Investigations of the New Madrid, Missouri, earthquake region: U.S. Geological Survey Professional Paper 1236, Chapter F.
8. Hopper, M. G., Algermissen, S. T., and Dobrovolsky, E. E., 1983, Estimation of earthquake effects associated with a great earthquake in the New Madrid seismic zone: U.S. Geological Survey, Open-file report 83-179, 94 p.
9. Housner, G. W., 1958, The mechanism of sandblows: Bulletin of the Seismological Society of America, v. 48, p. 155-161.
10. Keefer, D. K. (in press), Landslides caused by earthquakes: Geological Society of America Bulletin.
11. Krinitzsky, E. L., and Marcuson, W. F., 1983, Principles for selecting earthquake motions in engineering design: Bulletin of the Association of Engineering Geologists, v. xx, no. 3, p. 253-265.
12. Kuribayashi, E., and Tatsuoka, F., 1975, Brief review of liquefaction during earthquakes in Japan: Soils and Foundations, v. 15, no. 4, p. 81-92.
13. Mosaic, July/August, 1979, When soils start to flow, v. 10, no. 4, p. 26-34.

14. Nuttli, O. W., 1979, Seismicity of the central United States: in Geology in the siting of nuclear power plants; Reviews in Engineering Geology (Hatheway, A. W., and McClure, C. R. Jr., eds.), v. 4, The Geological Society of America, p. 67-93.
15. Nuttli, O. W., 1981, Evaluation of past studies and identification of needed studies of the effects of major earthquakes occurring in the New Madrid fault zone: A report submitted to Federal Emergency Management Agency Region VII, Kansas City, Missouri, 28 p.
16. Nuttli, O. W., 1983, Empirical magnitude and spectral scaling relations for mid-plate and plate-margin earthquakes: in Quantification of earthquakes (Duda, S. J., editor; et. al.), Tectonophysics, v. 93, no. 3-4, p. 207-223.
17. Nuttli, O., and Herrmann, R. B., 1978, State-of-the-art for assessing earthquake hazards in the United States--Credible earthquakes for the central United States: U.S. Corps of Engineers, Papers 5-13-1, report 12, 99 p.
18. Nuttli, O. W., and Herrmann, R. B., 1981, Consequences of earthquakes in the Mississippi Valley: Preprint 81-519, American Society of Civil Engineers, Conference at St. Louis, Missouri, Oct. 26-31, 1981, 13 p.

19. Nuttli, O. W., and Herrmann, R. B., 1982, Earthquake magnitude scales: American Society of Civil Engineers Proceedings, Journal of the Geotechnical Engineering Division, v. 103, no. GT 5, p. 783-786.
20. Powell, B. F., 1975, History of Mississippi County, Missouri, beginning through 1972: BLN Library Service, Independence, Missouri.
21. Russ, D. P., 1982, Style and significance of surface deformation in the vicinity of New Madrid, Missouri: in McKeown, F. A. and Pakiser, L. C., ed., Investigations of the New Madrid, Missouri, earthquake region: U.S. Geological Survey Professional Paper 1236, Chapter H.
22. Saucier, R. T., 1964, Geological Investigation of the St. Francis Basin, lower Mississippi Valley: U.S. Army Corps of Engineers, Waterways Experiment Station Technical Report 3-659.
23. Saucier, R. T., 1974, Quaternary geology of the lower Mississippi Valley: Arkansas Archeological Survey, Research Series No. 6, 26 p.
24. Saucier, R. T., 1977, Effects of the New Madrid earthquake series in the Mississippi alluvial valley: U.S. Army Engineer Waterways Experiment Station, Miscellaneous paper S-77-5, 10 p.

25. Seed, H. B., 1968, Landslides during earthquakes due to soil liquefaction: American Society of Civil Engineers Proceedings, Journal of the Soil Mechanics and Foundations Division, v. 93, no. SM 5, p. 1055-1122.
26. Seed, H. B., 1979, Soil liquefaction and cyclic mobility for level ground during earthquakes: American Society of Civil Engineers Proceedings, Journal of the Geotechnical Engineering Division, v. 105, no. GT2, p. 201-255.
27. Seed, H. B., and Idriss, I. M., 1971, Simplified procedure for evaluating soil liquefaction potential: American Society of Civil Engineers Proceedings, Journal of the Soil Mechanics and Foundations Division, v. 97, no. SM9, p. 1249-1273.
28. Seed, H. B., and Idriss, I. M., 1982, Ground motions and soil liquefaction during earthquakes: Earthquake Engineering Research Institute; Monograph series: Engineering monographs on earthquake criteria, structural design, and strong motion records; Berkeley, California, 134 p.
29. Seed, H. B., Idriss, I. M., and Arango, I., 1983, Evaluation of liquefaction potential using field performance data: American Society of Civil Engineers Proceedings, Journal of the Geotechnical Engineering Division, v. 109, no. 3, p. 458-482.

30. Seed, H. B., Idriss, I. M., Makdisi, F., and Bannerjee, N. 1975, Representation of irregular stress time histories by equivalent uniform stress series in liquefaction analyses: Earthquake Engineering Research Center, University of California, Berkeley, California, Report no. EERC 75-28, 13 p.
31. Sharma, Sunil; and Kovacs, W. D., 1980, Microzonation of the Memphis, Tennessee, area: Report no. 14-08-0001-17752, Purdue University, West Lafayette, Indiana, 129 p.
32. Smith, F. L. and Saucier, R. T., 1971, Geological investigations of the Western Lowlands area, lower Mississippi valley: U.S. Army Engineer Waterways Experiment Station, Corps of Engineers, Vicksburg, Mississippi, Technical Report No. S-71-5.
33. Stauder, W., 1982, Present day seismicity and identification of active faults of the New Madrid seismic zone: in McKeown, F.A. and Pakiser, L. C., eds., Investigations of the New Madrid, Missouri, earthquake region: U.S. Geological Survey Professional Paper 1236, Chapter C.
34. Tokimatsu, K., and Yoshima, Y., 1981, Field correlation of soil liquefaction with SPT and grain size: Proceedings of International Conference on Recent Advances in Geotechnical Earthquake Engineering and Soil Dynamics, University of Missouri-Rolla, April 26 - May 3, 1981, v. 1, p. 203-208.

35. Youd, T. L., 1973, Liquefaction, flow, and associated ground failure: U.S. Geological Survey Circular 688, 12 p.
36. Youd, T. L., 1977, Discussion of brief review of liquefaction during earthquakes in Japan by Eiichi Kuribayashi and Fumio Tatsuoka, 1975, in (Soils and Foundations, v. 15, no. 4, p. 81-92): Soils and Foundations, v. 17, no. 1, p. 82-85.
37. Youd, T. L., 1978, Major cause of earthquake damage is ground failure: Civil Engineering, American Society of Civil Engineers, v. 48, no. 4, April, p. 47-51.
38. Youd, T. L., and Bennett, M. J., 1983, Liquefaction sites, Imperial Valley, California: American Society of Civil Engineers Proceedings, Journal of the Geotechnical Engineering Division, v. 109, no. 3, p. 440-457.
39. Youd, T. L., and Hoose, S. N., 1978, Historic ground failures in northern California triggered by earthquakes: U.S. Geological Survey Professional Paper 993, 177p.
40. Youd, T. L., and Perkins, D. M., 1978, Mapping liquefaction-induced ground failure potential: American Society of Civil Engineers Proceedings, Journal of the Geotechnical Engineering Division, v. 104, no. GT4, p. 433-446.

Table 1. Ground slope and expected failure mode of coarse-grained deposits liquefied during earthquakes (after Youd, 1978).

Ground Surface Slope	Failure Mode
<hr/>	
<0.5%	Bearing capacity
0.5 - 5.0%	Lateral spread
>5.0%	Flow landslide

Table 2. Modified penetration resistance values (N_1) ^{1/} in selected setting in Western Lowlands and St. Francis Basins

Geologic-geographic setting	Median N_1	Lower Quartile N_1
Braided stream terrace deposits, Western Lowlands	22-23	15
Braided stream terrace deposits, southern half, St. Francis Basin	26	19
Meander belt deposits of Mississippi River	25	17-18

^{1/} N_1 is the modified penetration resistance of Seed and others (1983).

Table 3. Field boring log data at selected locations in Western Lowlands and St. Francis Basins.

Western Lowlands Basin

Boring log no. 266							Boring log no. 267						
Sample		Stratum		Field classification and remarks	N ₁ 2/ adjusted	N ₁ 3/ adjusted	Sample		Stratum		Field classification and remarks	N ₁	N ₁ adjusted
From (ft)	To (ft)	From (ft)	To (ft)				From (ft)	To (ft)	From (ft)	To (ft)			
		0.0	13.5	silty clay.					0.0	12.0	clayey silt.		
15.0	16.5	13.5		thin lenses of f and m and silty sand, and 1 in. lens of clay silt.	12	19-20			12.0	16.0	sandy silt, w/tr clay.		
									16.0		f sand.	11	18-19
18.0	19.5			m sand.	37	37	16.0	17.5			f and m sand.	18	18
21.0	22.5			f and m sand.	15	15	19.0	20.5			f and m sand.	20	20
24.0	25.5			f and m sand.	29	29	22.0	23.5			f and m sand.	24	24
27.0	28.5			f and m sand.	20	20	25.0	26.5			f and m sand, w/ some 1/16. in. lenses of clayey silt.	16	16
30.0	31.5			f and m sand.	30	30	28.0	29.5					
33.0	34.5	>34.5		f and m sand.	29	29	31.0	33.5			f and m sand.	12	12
							35.0	36.5	>36.5		f and m sand.	18	18

St. Francis Basin

Boring log no. 268							Boring log no. 269						
Sample		Stratum		Field classification and remarks	N ₁	N ₁ adjusted	Sample		Stratum		Field classification and remarks	N ₁	N ₁ adjusted
From (ft)	To (ft)	From (ft)	To (ft)				From (ft)	To (ft)	From (ft)	To (ft)			
		0.0	8.0	silty clay.					0.0	18.0	silty clay.		
		8.0	10.5	silt.			18.0	19.5	18.0		f sand, w/6 in. thick lens of sandy silt.	NA	NA
11.0	12.5	10.5		f sand.	12	19-20							
14.0	15.5			f sand.	41	48-49							
17.0	18.5			m sand in upper 6 in., layers of f to m sand in lower 12 in.	26	26	21.0	22.5			sandy silt.	NA	NA
				m sand, w/layers of 1/2 in. thick f sand.	56	56	24.0	25.5			lost sample.	NA	NA
20.0	21.5			m sand, w/lenses of f sand.	26	26	27.0	28.5			sandy silt, w/6 in. lens of clay.	NA	NA
23.0	24.5			m sand, w/gravel.	30	30	30.0	31.5			silty sand.	24	31-32
26.0	27.5			m sand, w/gravel.	67	67	33.0	34.5			clayey silt, w/6 in. lens of clay.	NA	NA
29.0	30.5			m sand, w/gravel.	63	63	36.0	37.5	≥ 37.5		sandy silt.	NA	NA
32.0	33.5	>37.5		m sand, w/gravel.									

(Table 3 continued on next page)

Table 3 (continued)

St. Francis Basin

Boring log no. 270

Sample		Stratum		Field classification and remarks	N ₁	N ₁ adjusted
From (ft)	To (ft)	From (ft)	To (ft)			
		0.0	9.0	silty clay.		
		9.0	11.0	sandy silt.		
10.0	11.5	11.0	11.5	lean clay.	NA	NA
		11.5	12.0	sandy silt.		
12.0	13.5	12.0	13.5	silty sand, w/very few thin clayey lenses.	NA	NA
		13.5	15.5	silty sand.		
15.0	16.5	15.5	16.0	f sand.	10	17-18
19.0	21.0	19.0	21.0	f and m sand.	9	9
21.0	22.5	21.0		f and m sand, w/ very thin clay lenses.	16	16
24.0	25.5	24.5	>25.5	f sand.	16	23-24

- 1/ The letters f and m are abbreviations for fine and medium, respectively.
- 2/ N₁ values are Standard Penetration Test (SPT) blow counts, adjusted for an overburden stress of 1 ton/ft².
- 3/ Where applicable, N₁ values are adjusted to account for influence of sand grain size on liquefaction potential, by adding 7 to 8 to values in adjoining column. Many of the sands classified in the field as being fine have an average diameter of about 0.25 mm, based on laboratory sieve testing of the composite sample from the SPT sampling tube. The samples' in-situ are typically alternating thin layers of very fine and fine to medium sand. Thus, adding 7 to 8 to the N₁ values for the samples designated as fine sand is conservative for back-calculating the 1811 accelerations.
- 4/ NA is abbreviation for 'not applicable' or 'not available'.

Table 4. Central Mississippi Valley historical earthquakes with body-wave magnitudes greater than 5.2, exclusive of 1811-12 earthquakes: locations, intensities, and liquefaction.

Location <u>1/</u>	Date	Modified <u>2/</u> Mercalli Intensity	Body-wave <u>1/</u> magnitude	Lique- faction <u>2/</u>
Miss. Embayment 35.2 N. Lat. 90.5 W. Long.	1-4-1843	VIII (minimum)	6.0	none reported
Miss. Embayment 36.5 N. Lat. 89.5 W. Long.	8-17-1865	VII	5.3	none reported
Miss. Embayment 37.0 N. Lat. 89.4 W. Long.	10-31-1895	VIII	6.2	common- place
Miss. Embayment 36.9 N. Lat. 89.3 W. Long.	11-4-1903	VII	5.3	none reported
Wabash Valley 39.0 N. Lat. 87.6 W. Long.	9-27-1909	VII	5.3	none reported
Miss. Embayment 35.5 N. Lat. 90.3 W. Long.	10-28-1923	VII	5.3	none reported
Miss. Embayment 36.5 N. Lat. 89.0 W. Long.	5-7-1927	VII	5.3	none reported
Wabash Valley 38.0 N. Lat. 88.5 W. Long.	11-9-1968	VII	5.5	none reported

1/ Reference: Nuttli and Herrmann, 1978.
2/ Reference: Coffman and von Hake, 1973.

Table 5. Suggested peak horizontal accelerations as a function of MM intensity, for New Madrid region earthquakes with surface-wave magnitudes (M_s) ≥ 7.0 .

<u>Location</u>	<u>MM intensity</u>		
	VII <u>1/</u>	VIII <u>1/</u>	X <u>2/</u>
Far field, hard site	0.09g	0.13g	0.20-0.25g
Far field, soft site	0.10g	0.15g	no data
Far field, St. Francis Basin alluvium	no data	no data	0.20g

1/ Data from Krinitzsky and Marcuson (1983).

2/ Data from this report.

Table 6. Suggested peak horizontal accelerations as a function of MM intensity, for New Madrid region earthquakes with surface wave magnitudes (M_s) < 6.9 . Data from Krinitzsky and Marcuson (1983).

<u>Location</u>	<u>MM intensity</u>		
	VI	VII	VIII
Far field, hard site	0.07g	0.11g	no data
Far field, soft site	0.05g	0.12g	0.20g

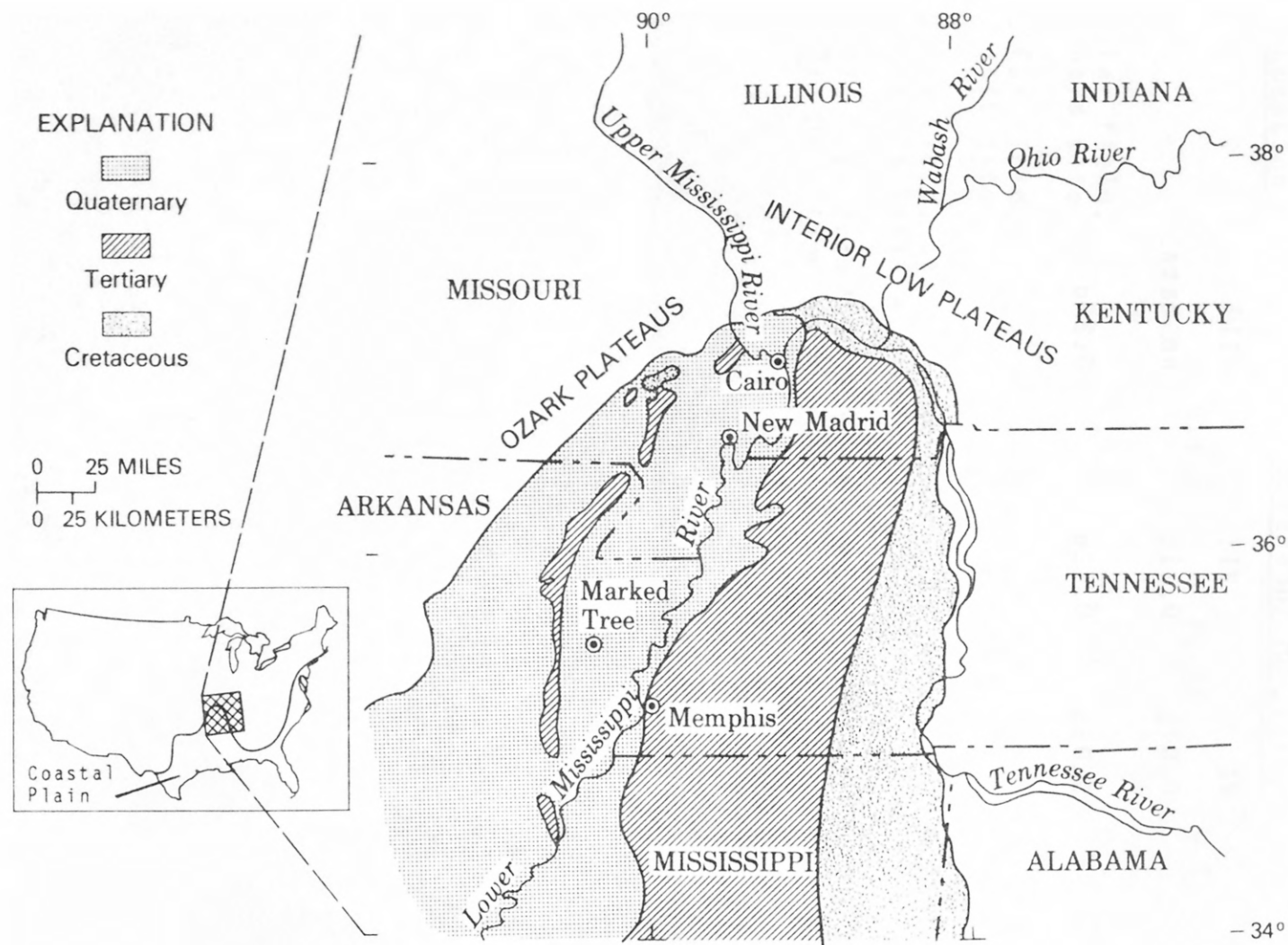


Fig. 1. Map of the northern Mississippi Embayment of the Gulf Coastal Plain, showing the major physiographic features of that area, and distribution of Quaternary alluvium, and Tertiary and Cretaceous sediments.

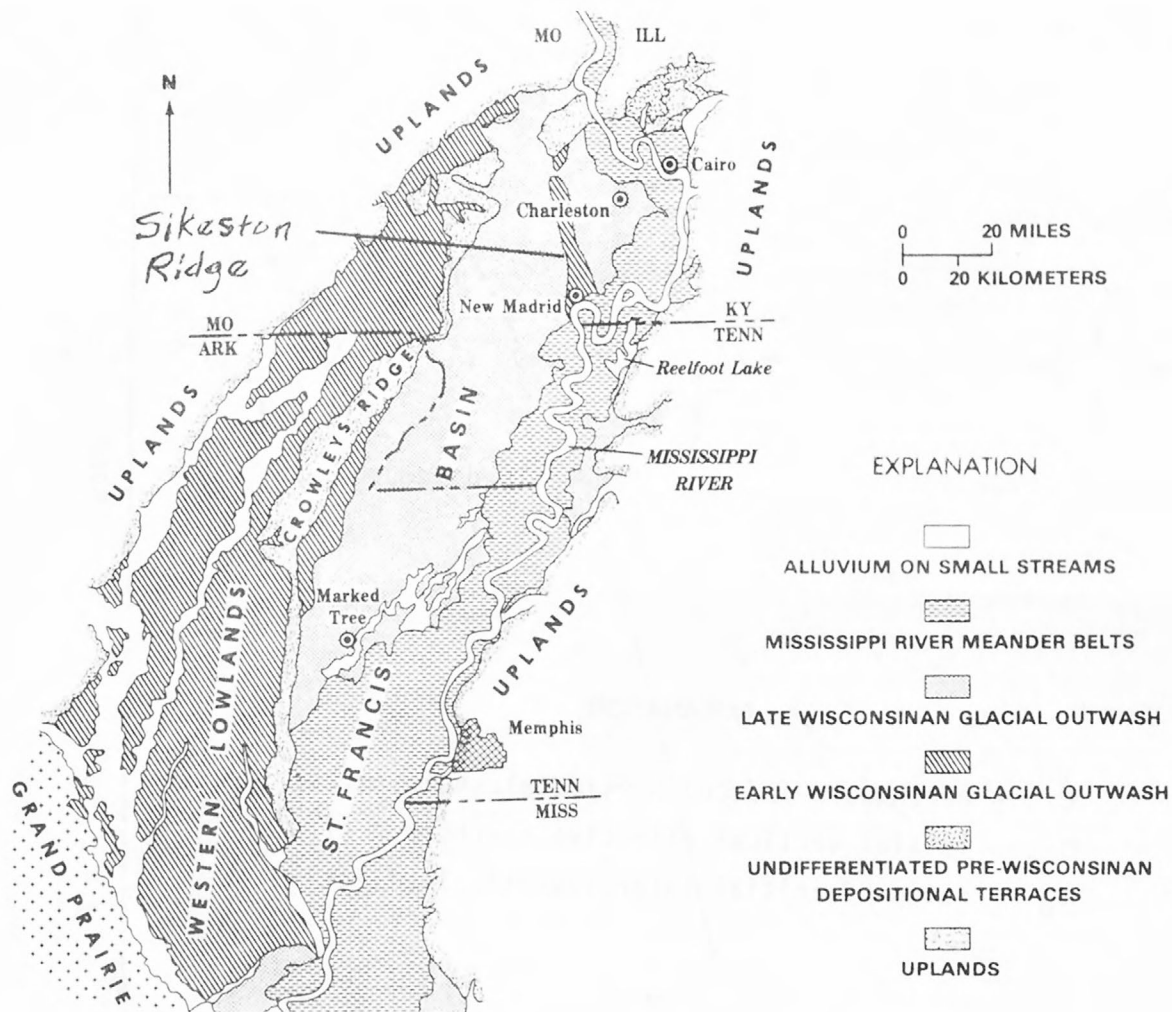
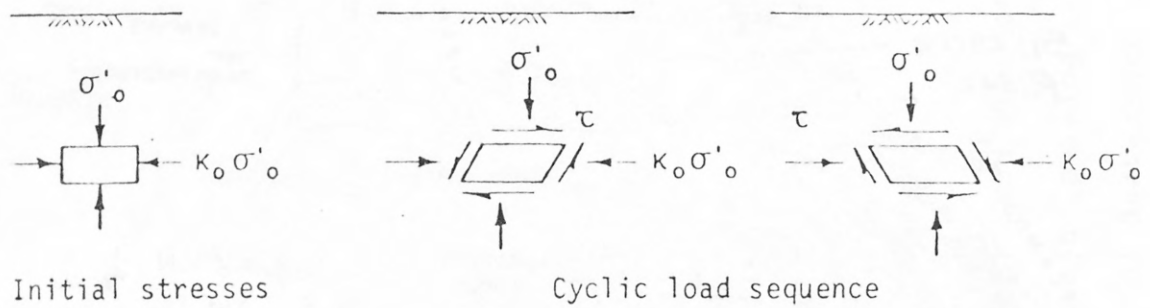


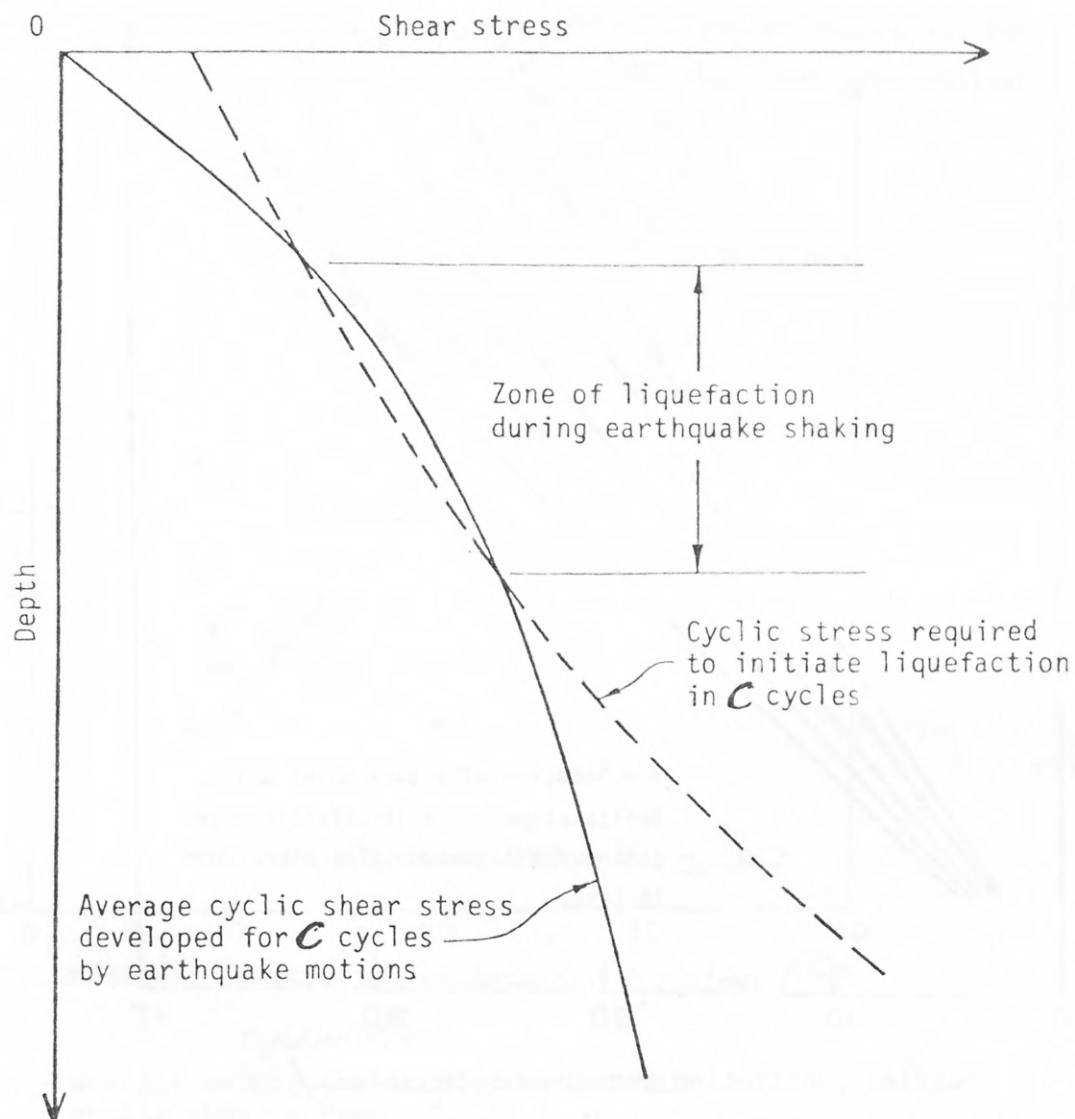
Fig. 2. Late Quaternary alluvial deposits in the St. Francis and Western Lowlands Basins (from Saucier, 1974).



EXPLANATION

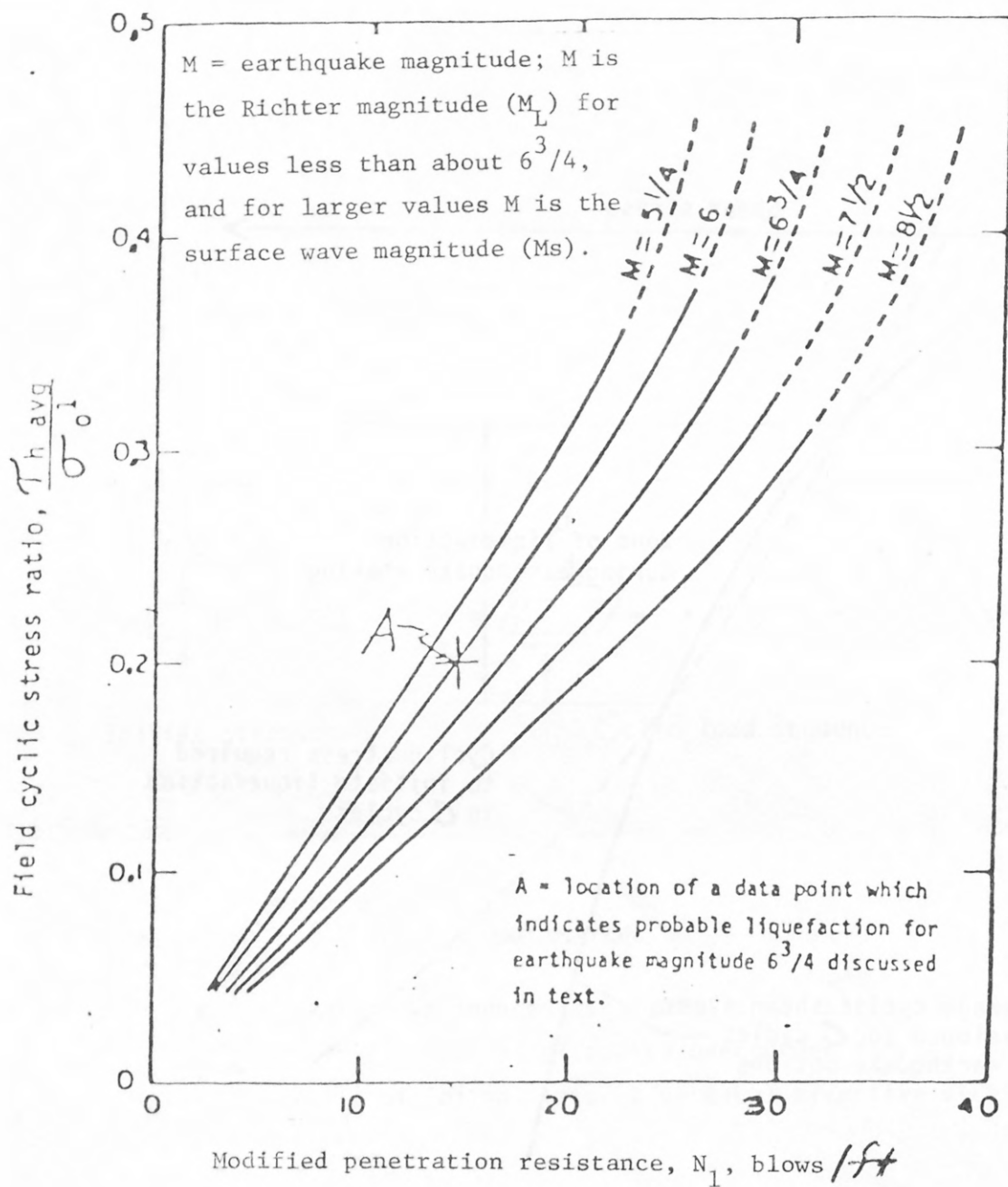
- τ - earthquake-induced horizontal shear stress
- σ'_o - initial vertical effective overburden stress
- κ_o - ratio of initial lateral/vertical effective stress

Fig. 3. Idealized field loading conditions (from Seed and Idriss, 1971).



C is the number of cycles

Fig. 4 Schematic depiction of the location of zone of liquefaction during earthquake shaking (from Seed and Idriss, 1971).



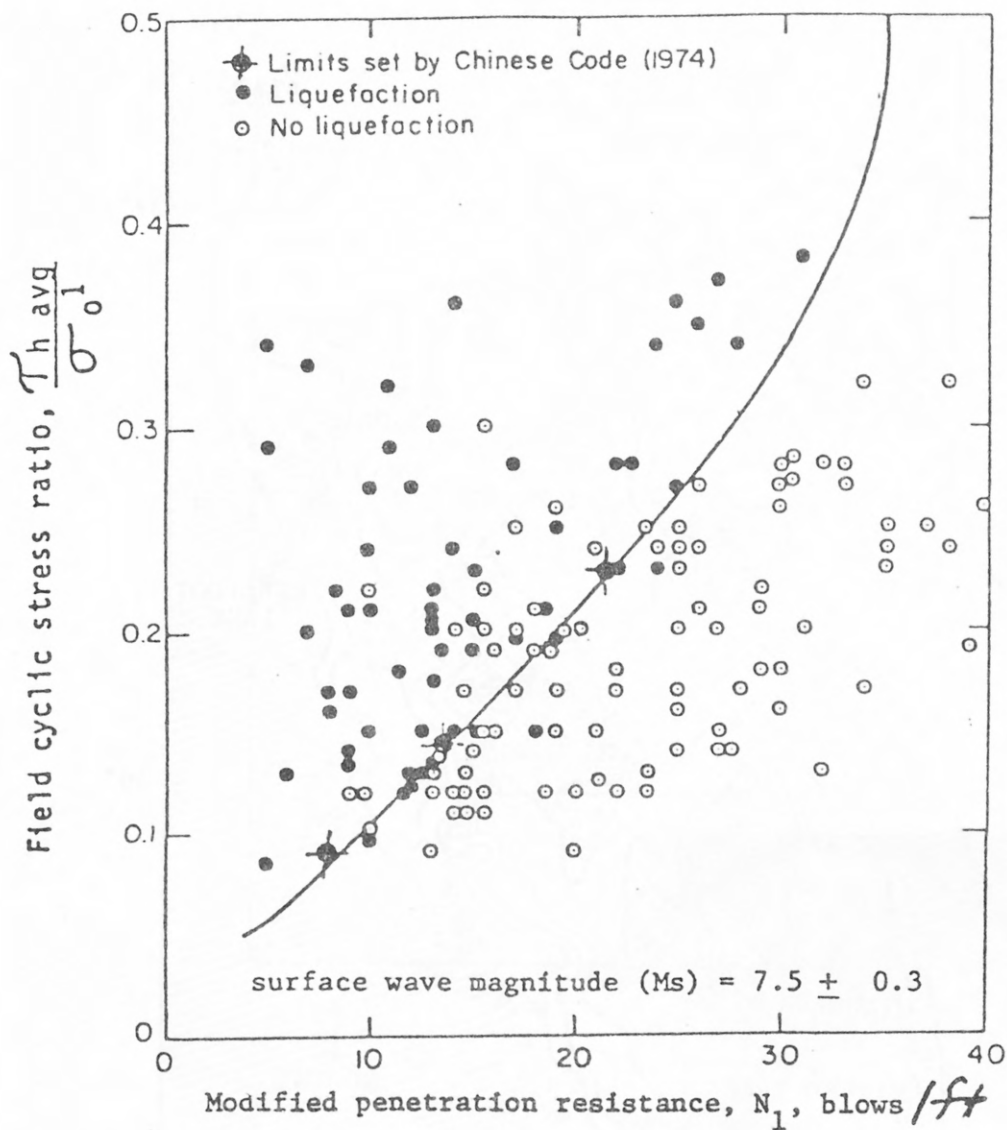
EXPLANATION

$T_{h \text{ avg}}$ - average earthquake-induced horizontal cyclic shear stress

σ_o' - vertical effective stress

N_1 - Standard Penetration Test blow count measured in field, modified to blow count resistance at vertical effective stress of 1 ton/ft²

Fig. 5. Chart for evaluation of liquefaction potential for different magnitude earthquakes (from Seed and others, 1983).



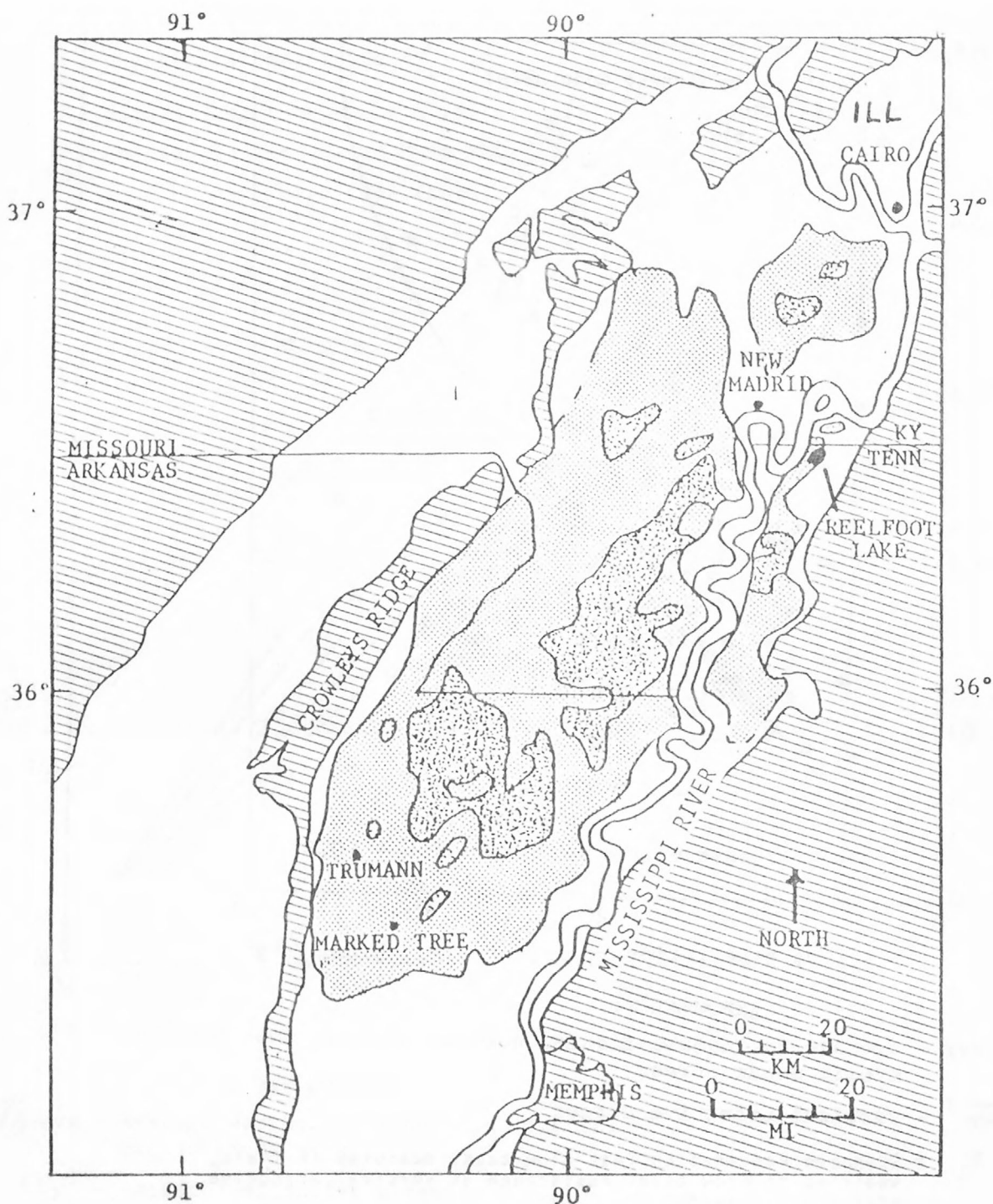
EXPLANATION

$T_h \text{ avg}$ - average earthquake-induced horizontal cyclic shear stress

σ_o1 - vertical effective stress

N_1 - Standard Penetration Test blow count measured in field, modified to blow count resistance at vertical effective stress of 1 ton/ft²

Fig. 6. Correlation between field liquefaction behavior of sands (average diameter > 0.25 mm) under level ground conditions and modified penetration resistance (from Seed and Idriss, 1981).



EXPLANATION



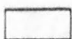

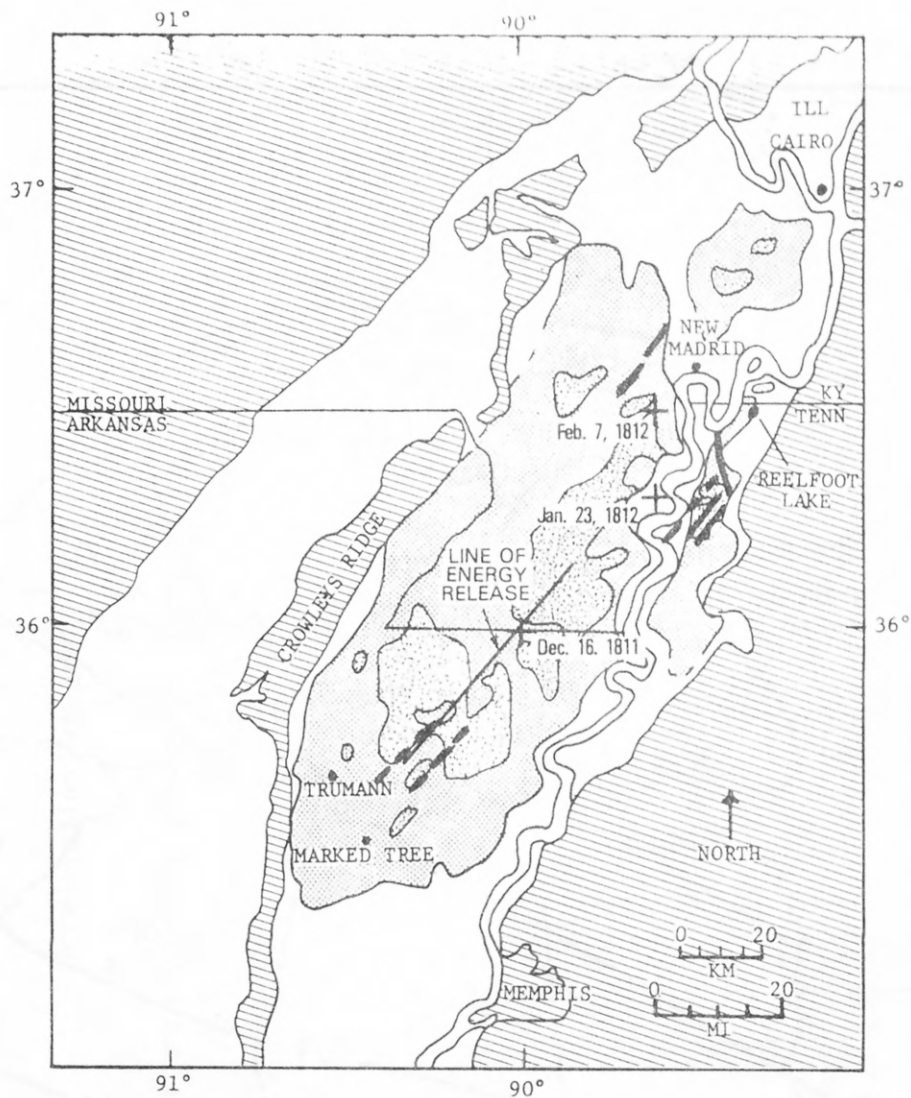


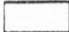



- | | | | |
|---|---|---|---|
|  | Upland areas |  | Wisconsin-age alluvium, with recognizable sand boil deposits but not intense ground coverage |
|  | Wisconsin-age alluvium, with no observed sand boils |  | Wisconsin-age alluvium, with more than 25 percent of ground surface covered by sand boil deposits |

Fig. 7. Distribution of sand boil deposits in Wisconsin-age alluvium, presumably produced by 1811-12 earthquakes.



EXPLANATION

- | | | | |
|--|---|---|---|
|  | Upland areas |  | Wisconsinan-age alluvium, with recognizable sand boil deposits but not intense ground coverage |
|  | Wisconsinan-age alluvium, with no observed sand boils |  | Wisconsinan-age alluvium, with more than 25 percent of ground surface covered by sand boil deposits |
| + Epicenters for earthquakes according to Nuttli (1979), on adjacent dates. | | | |
|  Fault zone | |  Fault | |

Fault zones and faults are from Hamilton and Zoback (1982).

Fig. 8. Energy release center line for the December 16, 1811 earthquake.

Explanation

The dashed horizontal line is the most probable peak horizontal acceleration in alluvium for the range in possible distances, A and B, from the epicenter of the December 16, 1811 earthquake; point C is the most probable distance. Point C' is the maximum possible peak horizontal acceleration in underlying bedrock at distance C.

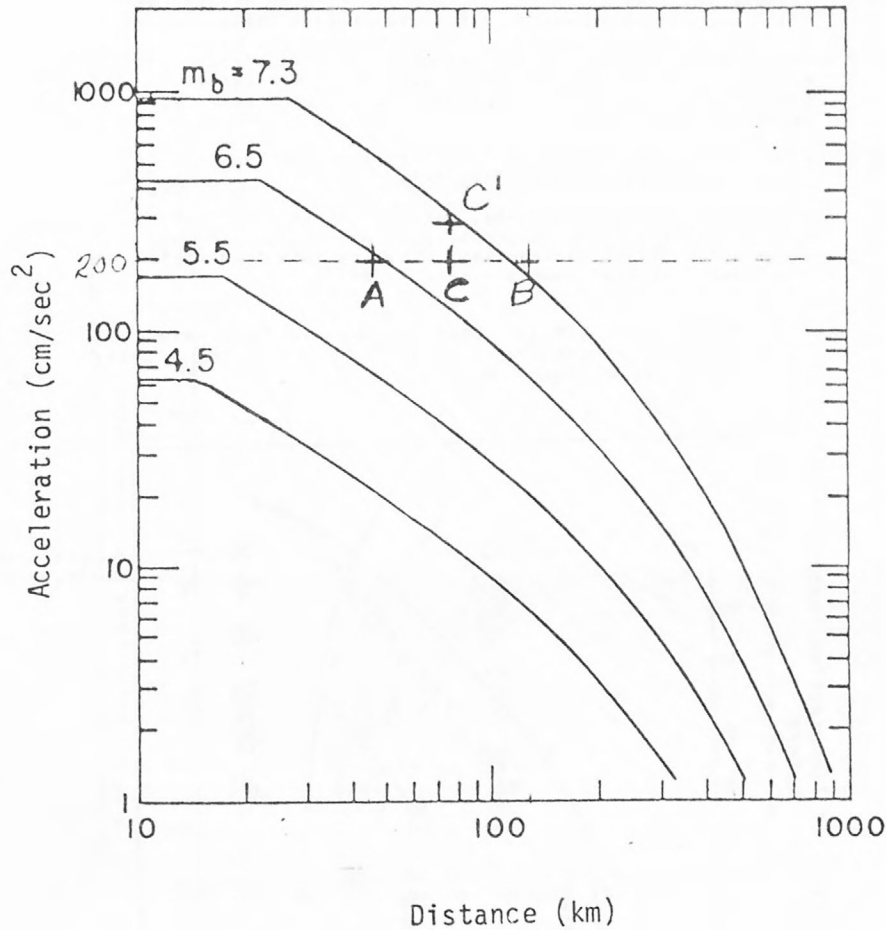


Fig. 10.--Peak horizontal acceleration in bedrock (average of two components) as a function of epicentral distance and body-wave magnitude (m_b) for the central United States (from Nuttli and Herrmann, 1981); and range of possible peak horizontal accelerations in alluvium. Distances from epicenter based on liquefaction data.

- outer limit of reported data, lateral spreads or flows, very probably > 40 mm movement, predominantly loose sediments, based on data from Davis and Berrill (1983) and Keefer (in press; personal communication, 1984); damage to poorly built structures.
- best fit for all data in Japan, outer limit of marginal liquefaction, predominantly loose sediments, by Kuribayashi and Tatsuoka (1975).
- outer limit on natural deposits for practical purposes, lateral spreads or flows, very probably > 40 mm movement, predominantly loose sediments, based on data from Davis and Berrill (1983) and Keefer (in press); damage to poorly built structures. Curve applies to N_1 values of 5 or less, and possibly higher.
- ⊙ data points, outer limits of sand boil deposits in St. Francis Basin alluvium exclusive of very young meander belt deposits along Mississippi River and small streams.
- conservative outer limit for marginal liquefaction, moderately thick sand deposits, data from this paper; damage to poorly built structures. Curve applies to N_1 values of 20 or less.
- X data point, outer limit of reported sand boil deposits for 1811-12 earthquakes, data from this paper.
- + outer limit of reported data, lateral spreads or flows, very probably > 40 mm movement, predominantly loose sediments, 1811-12 earthquakes, based on data from Keefer (in press; personal communication, 1984).

Magnitudes greater than 5.5 are surface wave magnitudes (M_s); values less than 5.5 are Richter local magnitudes (M_L).

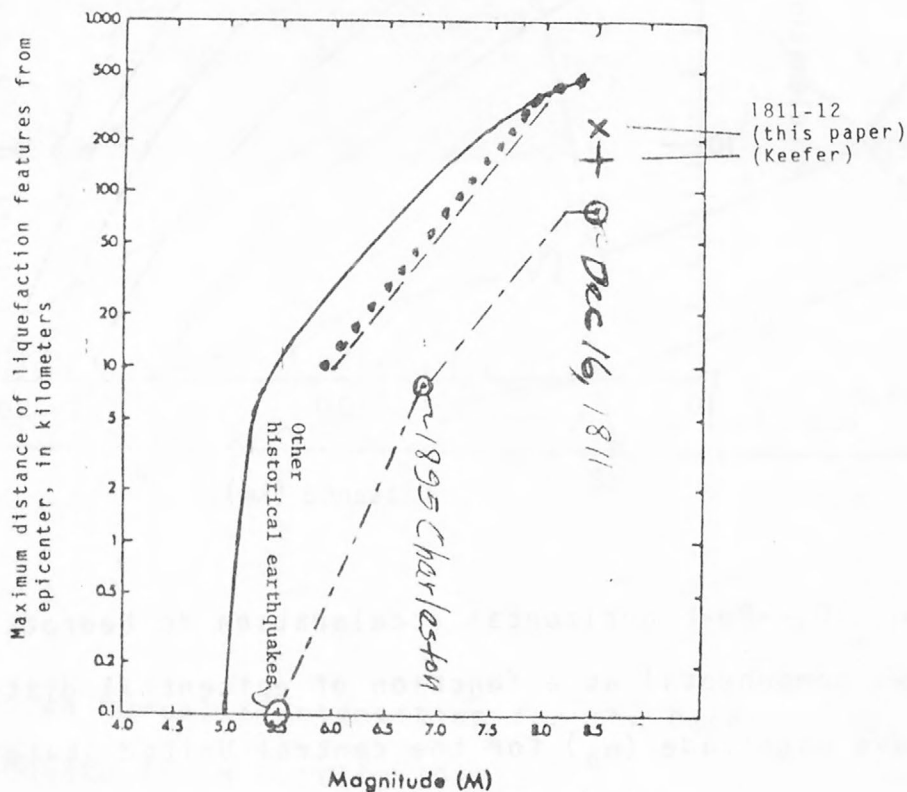


Fig. 11.--Maximum distance from epicenter of liquefaction in sand as a function of earthquake magnitude (part of this figure is modified from Keefer, in press).

Explanation

- outer limit of reported data, lateral spreads or flows, very probably > 40 mm movement, predominantly loose sediments, based on data from Keefer (in press; personal communication, 1984); damage to poorly built structures.
- - - practical outer limit, lateral spreads or flows, > 100 mm movement, predominantly loose sediments, by Youd and Perkins (1978); damage to most structures. Curve applies to N_1 values of 5 or less.
- ⊙ - - - ⊙ data points and practical outer limit for marginal liquefaction, moderately thick sand deposits, this paper; damage to poorly built structures. Curve applies to N_1 values of 20 or less.

Magnitude greater than 5.5 are surface wave magnitudes (M_s); values less than 5.5 are Richter local magnitudes (M_L).

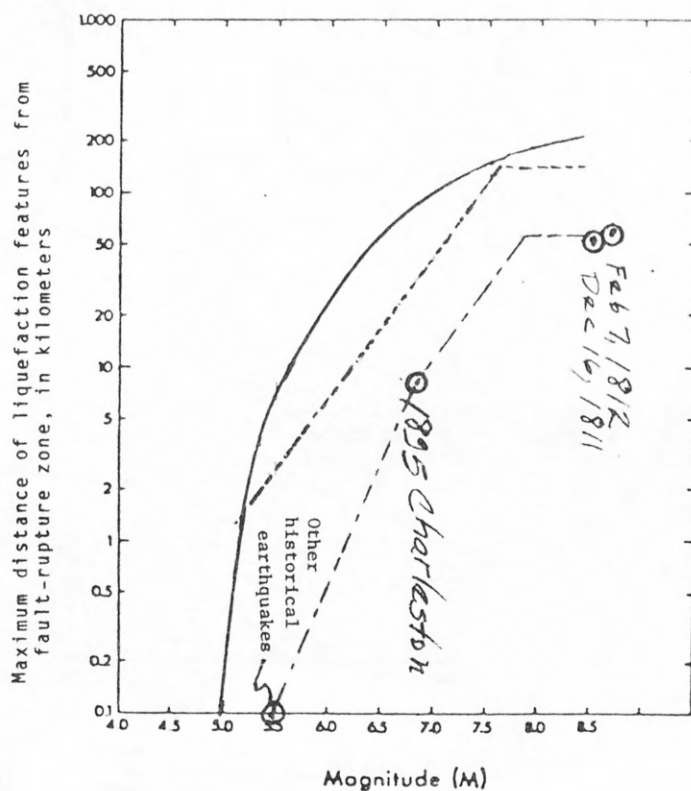


Fig. 12.--Maximum distance from fault-rupture zone of liquefaction in sand as a function of earthquake magnitude (part of this figure is modified from Keefer, in press).

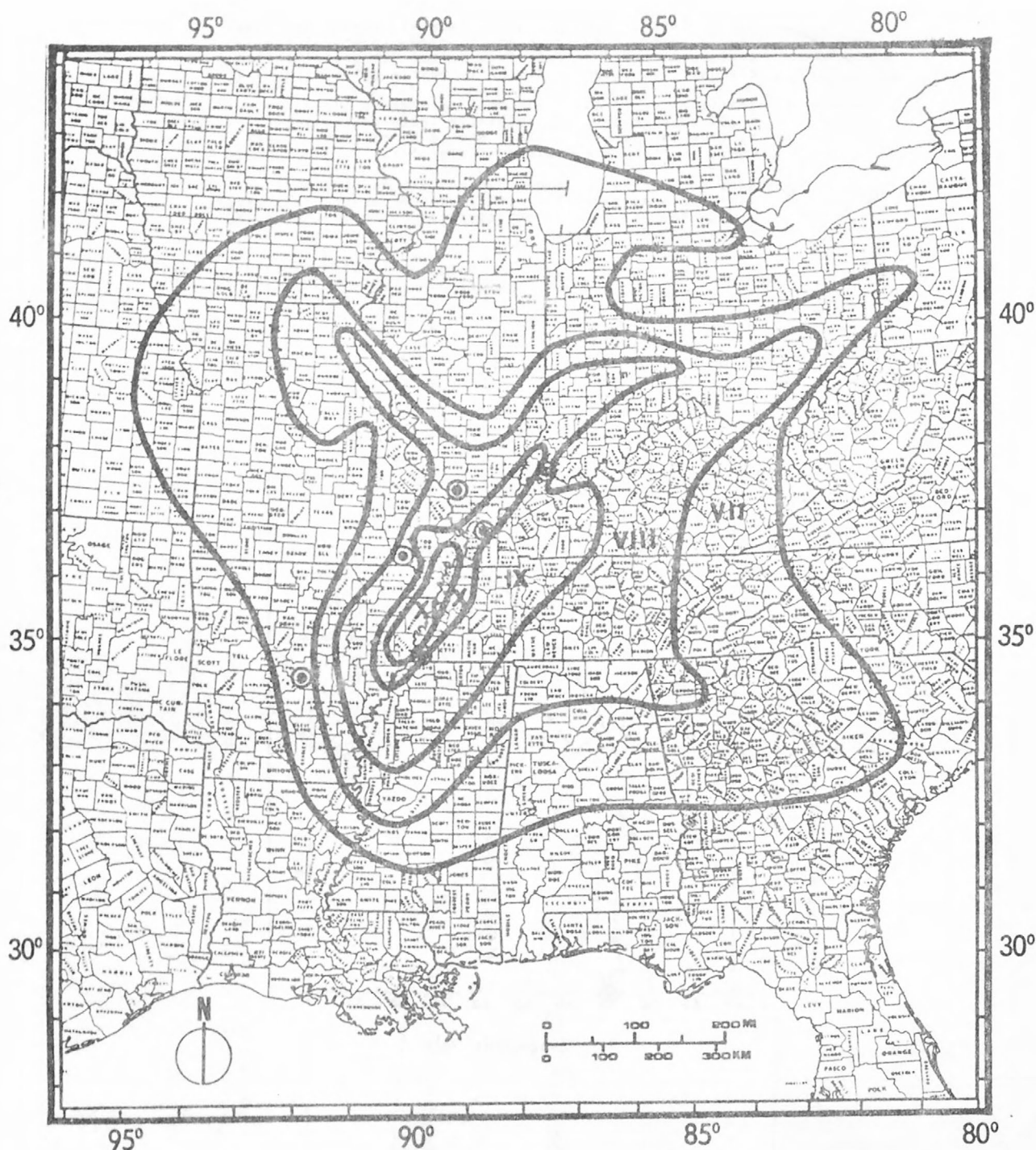


Fig. 13.--Hypothetical regional intensity map for an 1811-size earthquake having an epicenter anywhere along the New Madrid seismic zone (from Hopper and others, 1983). Intensities are highest that could be expected in a region, except where earthquake motions are unusually amplified or soils are unusually weak.

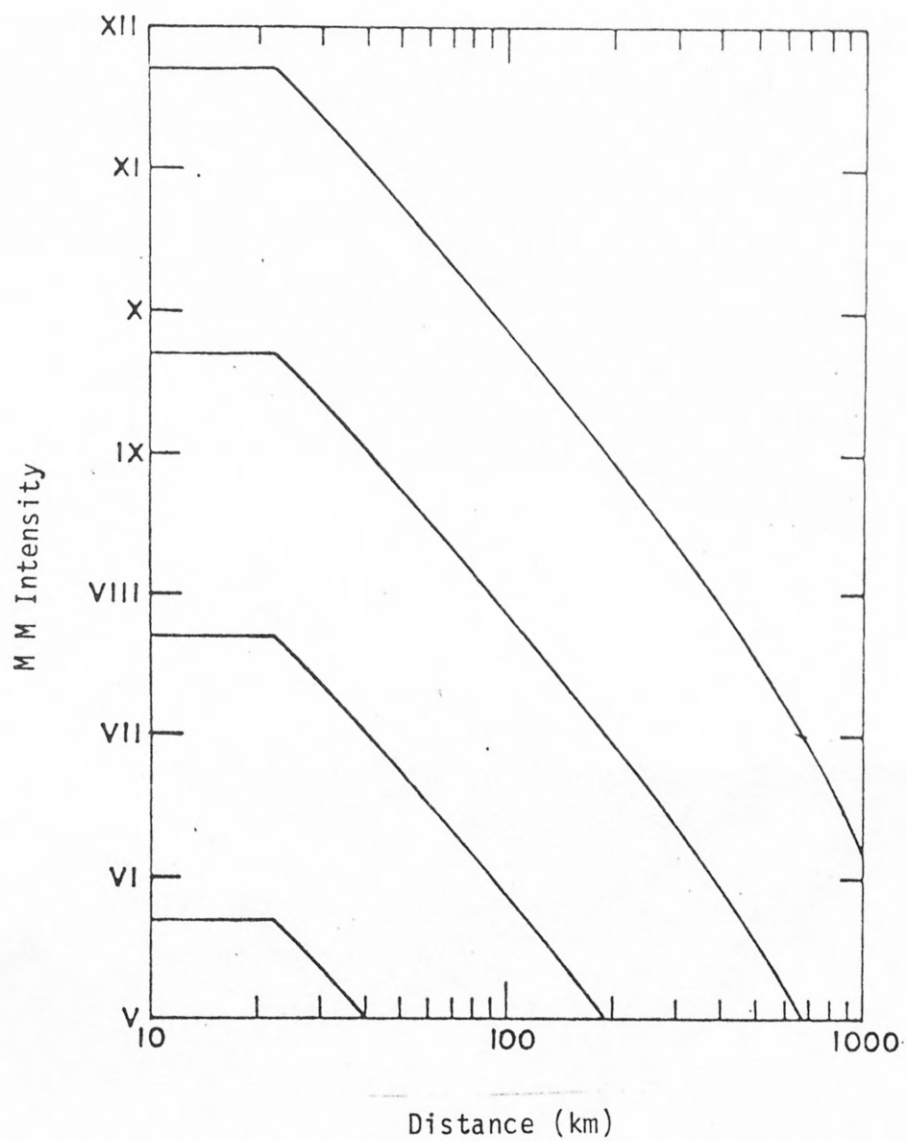


Fig. 14. Modified Mercalli intensity attenuation curves for the Central United States (from Nuttli, 1981).

USGS LIBRARY-RESTON



3 1818 00065207 1